

This is an Open Access document downloaded from ORCA, Cardiff University's institutional repository: <https://orca.cardiff.ac.uk/id/eprint/116964/>

This is the author's version of a work that was submitted to / accepted for publication.

Citation for final published version:

Carboni, Silvia, Zucca, Antonio, Stoccoro, Sergio, Maiore, Laura, Arca, Massimiliano, Ortu, Fabrizio, Artner, Christian, Keppler, Bernhard K., Meier-Menches, Samuel M., Casini, Angela and Cinellu, Maria Agostina 2018. New variations on the theme of gold(III) C^NN cyclometalated complexes as anticancer agents: Synthesis and biological characterization. *Inorganic Chemistry* 10.1021/acs.inorgchem.8b02604

Publishers page: <http://dx.doi.org/10.1021/acs.inorgchem.8b02604>

Please note:

Changes made as a result of publishing processes such as copy-editing, formatting and page numbers may not be reflected in this version. For the definitive version of this publication, please refer to the published source. You are advised to consult the publisher's version if you wish to cite this paper.

This version is being made available in accordance with publisher policies. See <http://orca.cf.ac.uk/policies.html> for usage policies. Copyright and moral rights for publications made available in ORCA are retained by the copyright holders.



New Variations on the Theme of Gold(III) C^NN Cyclometalated Complexes as Anticancer Agents: Synthesis and Biological Characterization

Silvia Carboni,^a Antonio Zucca,^{a,b} Sergio Stoccoro,^{a,b} Laura Maggiore,^a Massimiliano Arca,^c Fabrizio Ortu,^d Christian Artner,^{e,f} Bernhard K. Keppler,^{e,f} Samuel M. Meier-Menches,^{f,g} Angela Casini^{*,h} and Maria Agostina Cinellu^{*,a,b}

^a Dipartimento di Chimica e Farmacia, Università degli Studi di Sassari, via Vienna 2, 07100 - Sassari, Italy.

^b Consorzio Interuniversitario Reattività Chimica e Catalisi (CIRCC), 70126 Bari, Italy.

^c Dipartimento di Scienze Chimiche e Geologiche, Università degli Studi di Cagliari, S. S. 554 – bivio per Sestu, 09042 – Monserrato (Cagliari), Italy.

^d School of Chemistry, University of Manchester, Oxford Road, M13 9PL Manchester, United Kingdom.

^e Institute of Inorganic Chemistry, University of Vienna, Waehring Str. 42, 1090 Vienna, Austria.

^f Research Cluster “Translational Cancer Therapy Research”, University of Vienna, 1090 Vienna, Austria.

^g Department of Analytical Chemistry, University of Vienna, Waehring Str. 38, 1090 Vienna, Austria.

^h School of Chemistry, Cardiff University, Main Building, Park Place, CF10 3AT Cardiff, United Kingdom.

Corresponding authors' email address: casinia@cardiff.ac.uk , cinellu@uniss.it

Abstract

A series of novel (C^NN) cyclometalated Au^{III} complexes of general formula [Au(bipy^{dmb}-H)X][PF₆] (bipy^{dmb}-H = C^NN cyclometalated 6-(1,1-dimethylbenzyl)-2,2'-bipyridine) were prepared with a range of anionic ligands X in fourth coordination position, featuring either C- (alkynyl), N-, O- or S-donor atoms. The X ligands are varied in nature, and include three coumarins, 4-ethynylaniline, saccharine, thio-β-D-glucose tetraacetate, the tripeptide glutathione (GSH) and a coumarin-substituted amide derived from 4-ethynylaniline. The gold(I) complex [Au(C₂ArNHCOQ)(PPh₃)] (HC₂ArNHCOQ = *N*-(4-ethynylphenyl)-2-oxo-2*H*-chromene-3-carboxamide) was also prepared for comparison. The new compounds were fully characterized by means of analytical techniques, including NMR, absorption and emission spectroscopy. The crystal structures of three cyclometalated Au^{III} complexes and of the Au^I derivative were solved by single crystal X-ray diffraction. The antiproliferative activity of the new Au^{III} cyclometalated derivatives was evaluated against cancer cells *in vitro*. According to the obtained results, only complexes **3**-PF₆ and **5**-PF₆, featuring coumarins as ancillary ligands, and endowed with high redox stability in solution, display antiproliferative effects, with **5**-PF₆ being the most potent, while all the others are scarcely active to non-active in the selected cell lines. In order to study the reactivity of the compounds with biomolecules, the interaction of complexes **3**-PF₆ and **5**-PF₆ with the protein cytochrome c and the amino acids cysteine and histidine was analysed by electrospray ionization mass spectrometry (ESI MS), showing adduct formation only with Cys after at least 1 h incubation. Furthermore, the parent hydroxo complex [Au(bipy^{dmb}-H)(OH)][PF₆], **1OH**-PF₆, was investigated in a competitive assay to determine the protein vs. oligonucleotide binding preferences by capillary zone electrophoresis (CZE) coupled to ESI MS. Of note, the compound was found to selectively form adducts with the oligonucleotide over the protein upon ligand exchange with the hydroxido ligand. Adduct formation occurred within the first 10 min incubation, demonstrating the preference of **1OH**-PF₆ for nucleotides in this setup. Overall, the obtained results point towards the possibility to selectively target DNA with gold(III) organometallics.

INTRODUCTION

While the application of gold in medicine dates back to several thousand years, research into gold-based drugs has recently seen a renaissance.¹ Within this research area, organometallic gold complexes have been particularly explored as anticancer therapeutics, mainly due to their higher stability in physiological conditions guaranteed by the presence of a direct Au-C bond.¹⁻² In this context, Au^{III} complexes stabilized by C^N cyclometalated ligands represent a versatile class of organometallics which have found several applications due to their unique physicochemical properties³ that have been the subject of a number of investigations.⁴⁻⁶ Also intensely investigated are the applications of these complexes in the field of bioinorganic medicinal chemistry.^{2,7-9} Indeed, the superior stabilization of the gold(III) ion against reduction in aqueous solution, granted by C^N cyclometalated ligands with respect to, for example, N^N chelating ones, gave new impetus to the search of possible alternatives to platinum(II)-based anticancer agents. The first examples of cyclometalated Au^{III} complexes as potential anticancer agents were those based on the C^N ligand 2-(N,N-dimethylamino)methylphenyl.¹⁰⁻¹¹ Those complexes displayed higher cytotoxic activity than cisplatin against human cancer cells *in vitro* and antitumor activity comparable to the Pt(II) anticancer drug cisplatin *in vivo*.¹⁰⁻¹¹ Following these successful results, a number of other cyclometalated Au^{III} complexes supported by C^N chelates as well as by C^NN, N^CN and C^NC pincer ligands, endowed with promising anticancer properties and unique mechanisms of action, have been reported.^{2,7-9,12} These complexes also present the advantage of tolerating a large palette of ancillary ligands such as phosphanes,¹³⁻¹⁴ NHCs,¹⁵ and N-donor ligands,¹⁶ enabling optimization of their biological properties. In general, for such different families of gold(III) cyclometalated compounds, interactions with protein targets are considered to be responsible for their observed anticancer effects,^{9,17-18} whereas interactions with DNA seem less relevant, with a few exceptions.¹⁹⁻²⁰

Within this research area, several years ago some of us reported the synthesis and biological activity of the hydroxo complex [Au(bipy^{dmb}-H)(OH)][PF₆]²¹ (**1OH**-PF₆, bipy^{dmb}-H = C^NN cyclometalated 6-(1,1-dimethylbenzyl)-2,2'-bipyridine) and successively of other complexes derived from this precursor, namely the amido complexes [Au(bipy^{dmb}-H)(NHAr)][PF₆] (Ar = C₆H₄Me-4; C₆H₃Me₂-2,6),²² and the acetimidate complex [Au(bipy^{dmb}-H){NH(CO)Me}][PF₆].²³ The three compounds manifest rather similar chemical properties being stable in solution and moderately active in cancer cells.²²⁻²³ Reactions with proteins lead to formation of different amounts of metalated adducts, as evidenced by mass spectrometry, where a single {Au(bipy^{dmb}-H)} fragment is invariably linked to the protein.²³ Nevertheless, the reactivity of the compounds is different depending on the type of ancillary ligand used, with the acetimidate complex [Au(bipy^{dmb}-H){NH(CO)Me}][PF₆] being the least reactive.²³

In order to further explore the biological properties of this family of C^NN complexes, we report here on the synthesis, structural characterization and biological activity of new cyclometalated Au^{III} derivatives of general formula [Au(bipy^{dmb}-H)X]⁺ and a range of anionic ligands X in the fourth position, featuring either C-, N-, O- or S-donor atoms. The X ligands include three coumarins, 4-ethynylaniline, saccharinate, thio-β-D-glucose tetraacetate, the tripeptide glutathione (GSH) and a coumarin substituted amide, derived from 4-ethynylaniline, synthesized in this study. The gold(I) complex [AuX(PPh₃)], where X is the new ligand *N*-(4-ethynylphenyl)-2-oxo-2*H*-chromene-3-carboxamide, was also prepared for comparison.

The choice of coumarins was motivated by their pharmacological activities, including anticancer activity,²⁴ and for their photophysical properties. Coumarin fluorochromes are small and biocompatible, and are widely used for *in vivo* and *in vitro* diagnostics and imaging.²⁵⁻²⁶ As for saccharine, it was supposed to confer higher water solubility to the resulting complex and aspects of the biological profile of a number of saccharinate Au^I and Au^{III} complexes were investigated by some of us.²⁷ Thio-β-D-glucose tetraacetate is the ancillary ligand of the antiarthritic drug auranofin, the latter recently being investigated for potential therapeutic application in a number of other diseases including cancer, neurodegenerative disorders, HIV/AIDS, parasitic infections and bacterial infections.²⁸ Thus, this moiety has been widely used as ancillary ligand in a variety of metal-based drugs, due to its capability to facilitate uptake into cancer cells by modulating the lipophilic/hydrophilic character, as well as via possible interaction with GLUT1 transporters.²⁹⁻³⁰ Finally, the tripeptide glutathione is ubiquitous in cells where it exerts many roles: it acts as an antioxidant, a free radical scavenger and a detoxifying agent. Heavy metal ions are mainly removed by GSH after coordination to the thiol group. However, studies also postulated the role of GSH adduct formation in the mechanisms of toxicity of cisplatin;³¹ thus, the design of metal-GSH complexes could be exploited as a strategy to increase the anticancer effects of experimental metallodrugs. This notwithstanding, well defined GSH metal complexes are still rare.³²⁻³⁴

Thus, the new compounds were studied for spectroscopic properties, as well as for their antiproliferative effects in a small panel of human cancer cell lines and against non-tumorigenic cells from embryonic kidney (HEK-293) *in vitro*. In order to characterize the compounds with biological nucleophiles, some of the most cytotoxic derivatives were studied for their reactivity with the model protein cytochrome c (cyt c) and mixtures of amino acids by Electrospray Ionization Mass Spectrometry (ESI MS). Furthermore, capillary zone electrophoresis (CZE)–ESI MS allowed to determine the preference for the compounds' binding to a single strand oligonucleotide (5'-dATTGGCAC-3') in competition experiments with the model protein ubiquitin (ub).³⁵ For the first time, we observed some of the Au^{III} C^NN compounds to display remarkable affinity for nucleic acid binding, which may pave the way to the exploitation of these organometallic scaffolds to selectively target DNA structures.

RESULTS AND DISCUSSION

Synthesis and Characterization

The eight new cyclometalated Au^{III} compounds **2**-PF₆ to **9**-PF₆, of general formula [Au(bipy^{dmb}-H)X][PF₆] (where bipy^{dmb}-H = cyclometalated 6-(1,1-dimethylbenzyl)-2,2'-bipyridine, Figure 1) are characterized by a common terdentate C²N²N structural motif, while the anionic X ligands in the fourth position are varied in nature. These include: the deprotonated form of three commercially available coumarins, namely 2-oxo-2*H*-chromene-3-carboxylic acid (QCO₂H), 7-mercapto-4-methyl-2*H*-chromen-2-one (MeQSH) and 7-amino-4-(trifluoromethyl)-2*H*-chromen-2-one (CF₃QNH₂), and the coumarin substituted amide *N*-(4-ethynylaniline)-2-oxo-2*H*-chromene-3-carboxamide (HC₂ArNHCOQ) synthesized in this study, 4-ethynylaniline (HC₂ArNH₂), saccharine (Sacch), thio-β-D-glucose tetraacetate (GluSH) and the tripeptide glutathione (GSH).

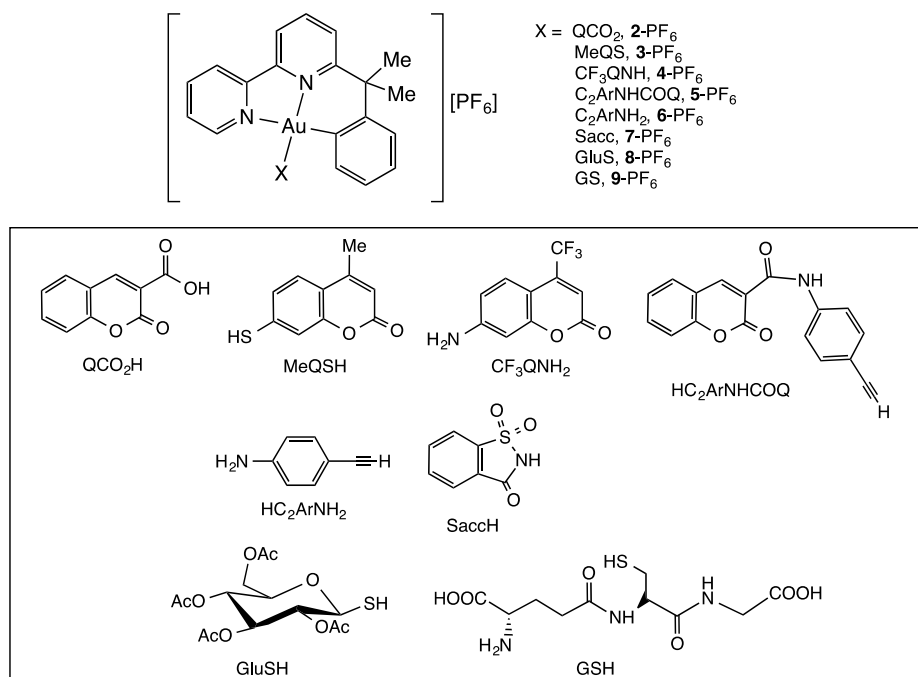
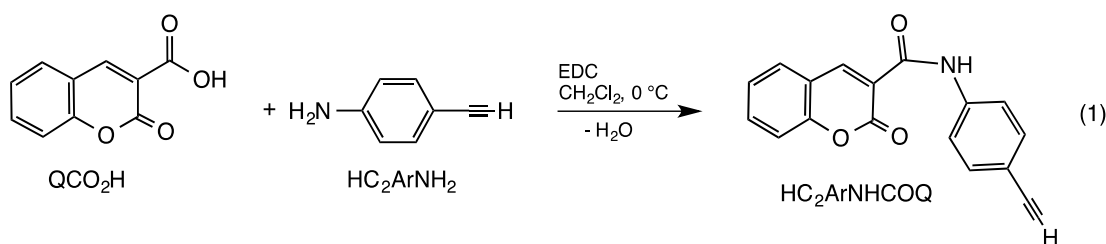


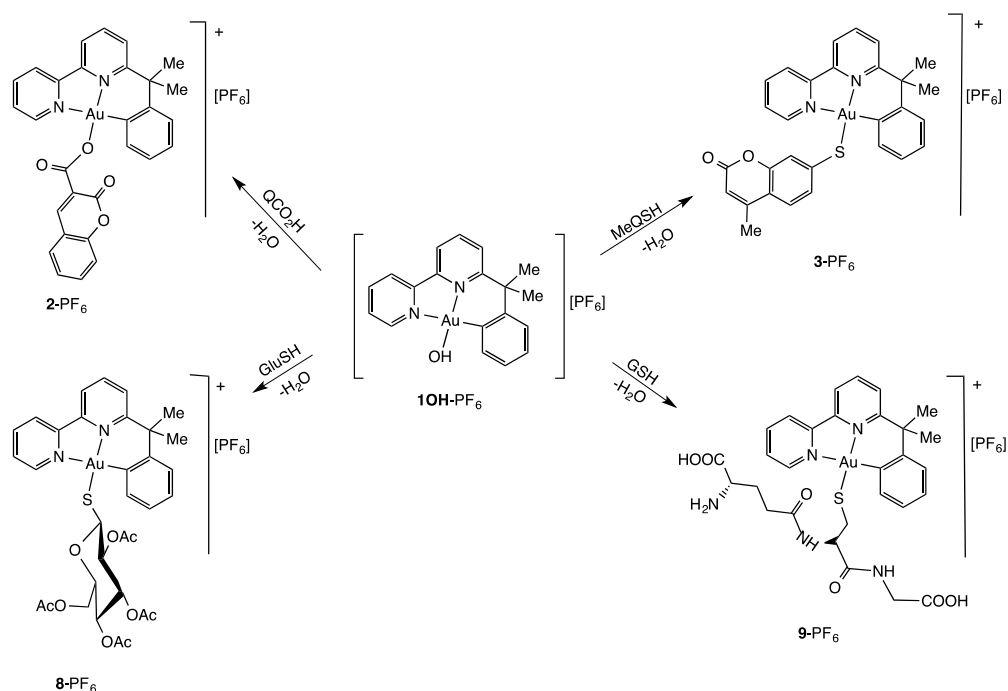
Figure 1. Structures of the Au^{III} complexes [Au(bipy^{dmb}-H)X][PF₆] **2**-PF₆ – **9**-PF₆.

The new ligand HC₂ArNHCOQ was obtained by condensation reaction of 4-ethynylaniline (HC₂ArNH₂) and coumarin-3-carboxylic acid (QCO₂H) in the presence of *N*-(3-dimethylaminopropyl)-*N*'-ethylcarbodiimide (EDC) as the coupling reagent (Scheme 1).



Scheme 1. Synthesis of the ligand $\text{HC}_2\text{ArNHCOQ}$ (*N*-(4-ethynylphenyl)-2-oxo-2*H*-chromene-3-carboxamide).

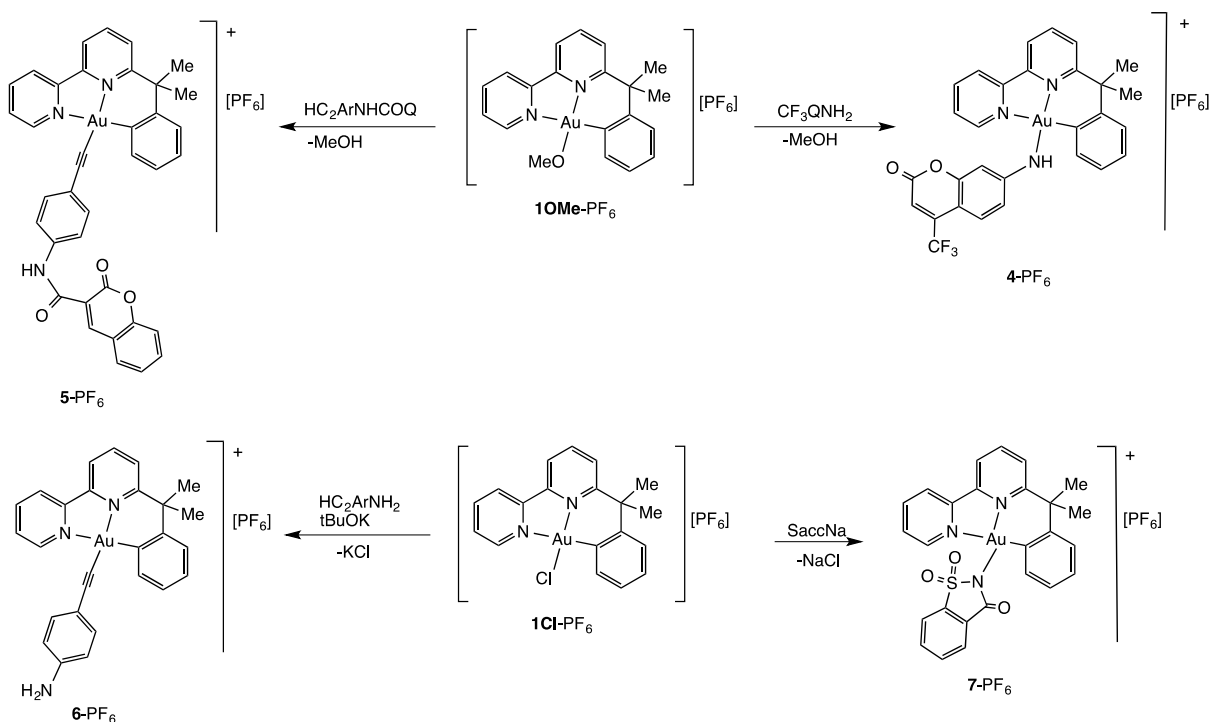
The new gold(III) complexes were obtained by σ -ligand metathesis reaction of the cyclometalated precursors $[\text{Au}(\text{bipy}^{\text{dmb}}\text{-H})\text{Y}][\text{PF}_6]$ $\{\text{Y} = \text{OH}$ (**1OH-PF₆**), OMe (**1OMe-PF₆**) or $\text{CH}_2\text{C}(\text{O})\text{Me}$ (**1CH₂Ac-PF₆**) $\}$ with the neutral HX ligand or from the chlorido complex $\{\text{Y} = \text{Cl}$ (**1Cl-PF₆**) $\}$ and the MX salt ($\text{M} = \text{Na}$ or K), depending on the acidity of the HX ligand (see Experimental section and Schemes 2 and 3). The precursors **1Y-PF₆** were synthesized as previously described by Cinellu et al.³⁶⁻³⁸



Scheme 2. Synthesis of complexes **2-PF₆**, **3-PF₆**, **8-PF₆**, and **9-PF₆** from the precursor **1OH-PF₆**.

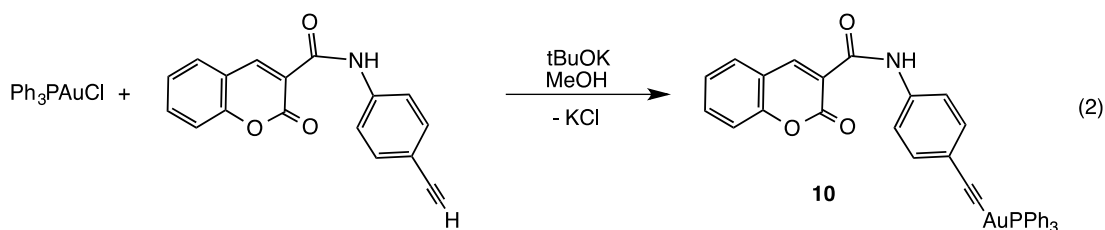
The reaction of the more acidic ligands QCO_2H , MeQSH , GluSH , and GSH with the hydroxo complex **1OH-PF₆** proceeds smoothly, in dichloromethane or aqueous solution (GSH), at room

temperature, to give, respectively, the carboxylato complex **2-PF₆** and the thiolato complexes **3-PF₆**, **8-PF₆** and **9-PF₆** in good yields. Under the same reaction conditions, and also in toluene at 80 °C, only small amounts of complex **5-PF₆** were obtained from reaction with the less acidic ligand HC₂ArNHQ as the competitive condensation reaction of **1OH-PF₆** to give the dinuclear oxo-bridged complex [Au₂(μ-O)(bipy^{dmb}-H)₂][PF₆]₂³⁹ occurred more rapidly. To overcome this undesired side-reaction, the methoxy **1OMe-PF₆** or the acetyl **1CH₂Ac-PF₆** complexes were used as the cyclometalated precursors. The amido complex **4-PF₆** was obtained from the reaction of CF₃QNH₂ with **1OMe-PF₆** in CH₂Cl₂ at room temperature (Scheme 3). Unexpectedly, no reaction occurred between any of the **1Y-PF₆** (Y = OH, OMe or CH₂Ac) and HC₂ArNH₂, nevertheless the alkynyl complex **6-PF₆** could be obtained from reaction with the chlorido complex **1Cl-PF₆** in the presence of tBuOK in ethanol solution (Scheme 3). The saccharinate complex **7-PF₆** was obtained from reaction of SaccNa with **1Cl-PF₆** in water.



Scheme 3. Synthesis of complexes **5-PF₆** and **4-PF₆** from the precursor **1OMe-PF₆** and of **6-PF₆** and **7-PF₆** from the precursor **1Cl-PF₆**.

The gold(I) complex **10** was synthesized by reaction of [AuCl(PPh₃)] with the new ligand HC₂ArNHCOQ in methanol in the presence of tBuOK (Scheme 4).



Scheme 4. Synthesis of the Au^I complex **10**.

The new gold(III) cyclometalated complexes **2**-PF₆ – **9**-PF₆ and the gold(I) complex **10** are fairly stable both in the solid state and in solution and were fully characterized by means of analytical and spectroscopic techniques. With the exception of the water-soluble glutathione derivative **9**-PF₆, all the complexes are soluble only in organic solvents. The FT-IR spectra recorded in the range 4000–600 cm⁻¹ show the peaks that are attributed to the cyclometalated bipy^{dmb} ligand and to the ancillary ligands. The NMR (¹H), IR and UV-vis spectroscopic data of the gold(III) complexes **2**-PF₆ – **9**-PF₆ and for the gold(I) complex **10** are listed in the Experimental section and are consistent with the expected structures, which for complexes **2**-PF₆, **3**-PF₆, **6**-PF₆ and **10** were confirmed by single-crystal X-ray analysis (see below).

The ¹H NMR spectrum of each complex (Figures S1–S12) shows the resonances of the cyclometalated bipy^{dmb} and the ancillary ligand in the expected 1 : 1 integral ratio. In all cases, the signal of the H⁶ proton (numbering scheme as in the Experimental), *i.e.* that in proximity of the ancillary ligand, is the most deshielded one (with the exception of the NH of complex **5**-PF₆), and the most sensitive to the donor atom of the ancillary ligand, as usually observed for this kind of complexes.³⁶⁻³⁸ Within this series, the highest downfield shifts (with respect to the free ligand) are observed for complexes **5**-PF₆ and **6**-PF₆, both featuring a C-donor ligand, followed by **3**-PF₆, **8**-PF₆ and **9**-PF₆, featuring an S-donor ligand. Moreover, the H^{3'} proton, in *ortho* position to the metalated carbon atom of the bipy^{dmb} ligand, undergoes a downfield shift, although to a lesser extent with respect to the H⁶.

In all cases, with the exception of complexes **8**-PF₆ and **9**-PF₆, only one set of signals is observed. Notably, complexes **5**-PF₆ and **6**-PF₆, whose ancillary ligands (HC₂ArNHCOQ and HC₂ArNH₂) possess two activable protons, *i.e.* N-H (amidic in the former and aminic in the latter) and methynic C-H, only the latter is activated leading to the alkynyl derivatives as shown by the absence of the signal of the methynic proton at 3.05 and 3.16 ppm in the free ligands. Two sets of signals are instead observed for complexes **8**-PF₆ and **9**-PF₆, with integral ratios of 1:0.2 and 1:0.1, respectively. In the case of the thio-glucose tetraacetate derivative **8**-PF₆, the two species are likely diastereomers due to the chiral nature of the ligand, and an analogous coordination behaviour was previously observed in the cyclometalated derivative [Au(py^b-H)(GluS)₂] (py^b-H = cyclometalated 2-benzylpyridine).¹³ In the case of complex **9**-PF₆,

due to the number of activatable protons, the two species are likely bond isomers: the major one being undoubtedly the S-bonded isomer while the minor species is likely an O-bonded derivative, as suggested by the very different chemical shifts of the H⁶ proton of the two isomers: 9.30 ppm (major species) and 8.74 ppm (minor species); these values are in line with those observed respectively for the S-donor and O-donor ligand derivatives (see above). Strong evidence of coordination to the deprotonated thiol group is provided by the resonance of methylene protons CH₂-5x that in the free ligand gives rise to one multiplet (due to coupling to SH and H^{4x}) at 2.95 ppm, while in the complex it appears as an AB quartet - with each signal further split by coupling with H^{4x} - centred at 3.13 ppm ($J_{AB} = 13.4$ Hz). Moreover, disappearance of the S-H stretching vibration at 2525 cm⁻¹ further supports deprotonation and coordination of the thiol group. As shown by the ¹H and ³¹P{¹H} NMR spectra (Figure S13), only the alkynyl derivative was formed also in the case of the gold(I) complex **10**.

Acetonitrile solutions of all the new Au^{III} complexes **1Cl**-PF₆, **1OH**-PF₆, **1OMe**-PF₆, **2**-PF₆ - **9**-PF₆ and **10** feature peculiar UV-Vis absorption bands in the region between 220 and 350 nm (Table S1). An analysis of the absorption spectra recorded on solutions at concentrations systematically varied between 2.6·10⁻⁵ and 1·10⁻⁴ M does not show any evidence of intermolecular interactions. Most of the spectra of the gold(III) complexes display two or three groups of bands, falling at different energies:

(i) All the UV-Vis absorption spectra display an intense and broad UV band, whose maximum falls below 220 nm. According to what was established for Au^{III} square-planar complexes deriving from the 2-(2'-pyridyl)benzimidazole (pbiH) ligand,⁴⁰ this band could be tentatively attributed to the overlap of numerous singlet transitions, also involving low lying Molecular Orbitals (MOs) with significant contributions from the 5d Atomic Orbitals (AOs) of the gold metal ion.

(ii) The absorption bands in the range 240–330 nm, in many cases overlapped by the more intense UV absorption (see above), can be envisaged in the electronic spectra of the ligands and can be therefore attributed to interligand (IL) transitions.

(iii) All Au^{III} complexes display a band, featuring a maximum in the range 320–330 nm, at energies lower than those of the lowest energy bands of the relevant ligands. This band is significantly red-shifted to 410 nm in **4**-PF₆ (Figure 2). In agreement to previous theoretical results³⁶ and to what was previously proposed for **1Cl**-PF₆ and **1OH**-PF₆,²¹ this band features a partial Ligand-to-Metal Charge-Transfer (LMCT) character.

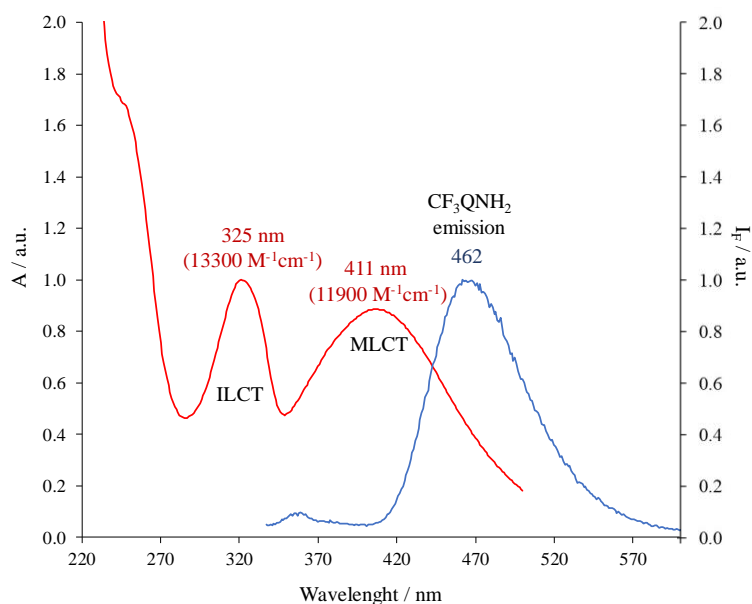


Figure 2. Overlay of the UV-Vis (220–500 nm) absorption spectrum (normalized on the peak at 325 nm; molar extinction coefficient in parentheses) and the normalized emission spectrum ($\lambda_{\text{exc}} = 325$ nm) recorded for **4**-PF₆ [$2.52 \cdot 10^{-5}$ M] in acetonitrile solution.

Concerning the neutral Au^I complex **10**, in addition to the intense UV absorption, whose tail can be seen in the range 220–260 nm, two sets of absorption band can be observed, namely a structured band, centered at 298 nm, and a very broad band (half-bandwidth 90 nm) at about 345 nm (Figure S14), that can be attributed to a MLCT transitions based on the DFT calculations carried out on the neutral complex [Au^I(pbi)Cl].⁴⁰

The emission properties of the synthesized complexes were measured at r.t. in acetonitrile solution (Table S1). The bipy^{dmb} ligand features a well-defined emission band at $\lambda_{\text{em}} = 384$ nm. All the complexes of the type [Au(bipy^{dmb}-H)X][PF₆] featuring a non-emissive ancillary ligand X (**1Cl**-PF₆, **1OH**-PF₆, **1OMe**-PF₆, **8**-PF₆, **9**-PF₆) display a single emission peak at about 350 nm, therefore being tentatively attributed to the perturbed emission of the bipy^{dmb} ligand. The same emission energy is shown by **6**-PF₆ (Table S1). Notably, the emission energy of these complexes matches that observed in diluted CH₂Cl₂ solution for [Au(bpi)Cl₂] and [Au(pbi)(AcO)₂] ($\lambda_{\text{em}} = 360$ nm), showing a common Au^{III}(N[^]N) coordination environment.⁴⁰ Since complexes **3**-PF₆ and **5**-PF₆, featuring emitting ancillary ligands, show similar emission properties ($\lambda_{\text{em}} = 374$ and 365 nm, respectively), it should be inferred that the peculiar emission of the coumarin-based ancillary ligands ($\lambda_{\text{em}} = 381$ and 465 nm for MeQSH and HC₂ArNHCOQ, respectively) would be quenched upon coordination to the metal ion. The typical emission of coumarin is instead preserved in the case of the complexes **2**-PF₆ (Figure S15) and **4**-PF₆ (Figure 2), which show low-energy emission bands in the visible region ($\lambda_{\text{em}} = 410$ and 462 nm, respectively) at roughly the same energy as the uncoordinated ligands ($\lambda_{\text{em}} =$

415 and 470 nm for QCO₂H and CF₃QNH₂, respectively). Similarly, complexes **7**-PF₆ and **10** (Table S1 and Figure S16) feature emission bands in the same wavelength range (435-470 nm) as the starting sodium saccharinate and HC₂ArNHCOQ precursors (λ_{em} = 440 and 460 nm, respectively). This suggests that the MOs of chromophores involved in the luminescence of the complexes **2**-PF₆, **4**-PF₆, **7**-PF₆, and **10** do not mix significantly with the AOs of the metal ion in the resulting complexes. In general, the emission intensity of the complexes is sensibly lower than that of the related free ligands.

The total or partial quenching of the emission of the ligands observed under coordination could be tentatively attributed to InterSystem Crossing (ISC). In line with what was discussed based on QM calculations carried out on different Au^{III} complexes,⁴⁰ the spin-forbidden ISC is induced by the interaction between the electronic spin and orbital moments. Since the spin-orbit coupling constant depends on the fourth power of the effective nuclear charge,⁴¹ ISC is increased in molecular systems containing heavy atoms, such as gold. ISC relies on the overlap between the vibrational wavefunctions of the initial (singlet) and the final (triplet) states, so that pairs of quasi-degenerate states of different spin multiplicity are good candidates to be involved in ISC processes, especially when ligands with a large degree of π -electron delocalization are present in the complexes. Consequently, ISC may provide an alternative relaxation path with respect to fluorescence, thus accounting for the lower emission featured by the complexes as compared to the corresponding emitting ligands.

Crystal Structures of Complexes **2**-PF₆, **3**-PF₆, **6**-PF₆ and **10**

For three of the Au^{III} complexes, namely [Au(bipy^{dmb}-H)(QCO₂)] [PF₆], **2**-PF₆, [Au(bipy^{dmb}-H)(MeQS)] [PF₆], **3**-PF₆, [Au(bipy^{dmb}-H)(C₂ArNH₂)] [PF₆], **6**-PF₆, and for the gold(I) complex [Au(C₂ArNHCOQ)(PPh₃)], **10**, the structure in the solid state was solved by X-ray diffraction analysis (see Table S2 for crystallographic details). X-ray quality crystals were obtained by slow diffusion of diethyl ether into a dichloromethane solution of complexes **2**-PF₆ and **10** and into an acetonitrile solution of complexes **3**-PF₆ and **6**-PF₆. ORTEP views of **2**-PF₆, **3**-PF₆ and **6**-PF₆ with the atom labelling schemes are shown in Figure 3 and selected bond lengths and angles collected in Table S3. In the gold(III) complexes the gold atom displays a tetrahedrally distorted square-planar coordination. Bond parameters involving the cyclometalated C^NN ligand can be compared with those found for the parent compound **1Cl**-AuCl₄³⁸ and for [Au(bipy^{dmb}-H)(SPh)] [PF₆].³⁷ Small but significant differences are found for the Au-N2 bond lengths of the three complexes due to the different *trans*-influence of the donor atom of the *trans*-disposed ancillary ligand. The six-membered metallacycle Au1-N2-C10-C11-C12-C17 in **2**-PF₆, **3**-PF₆ and **6**-PF₆ is in a boat conformation and the phenyl ring and the two pyridine rings are not coplanar; the methyl in axial position points to the metal centre with Au1 ... H18A

distances of 2.647, 2.576 and 2.853 Å, respectively, that is less than the sum of Au (1.80 Å) and H (1.20 Å) van der Waals radii.

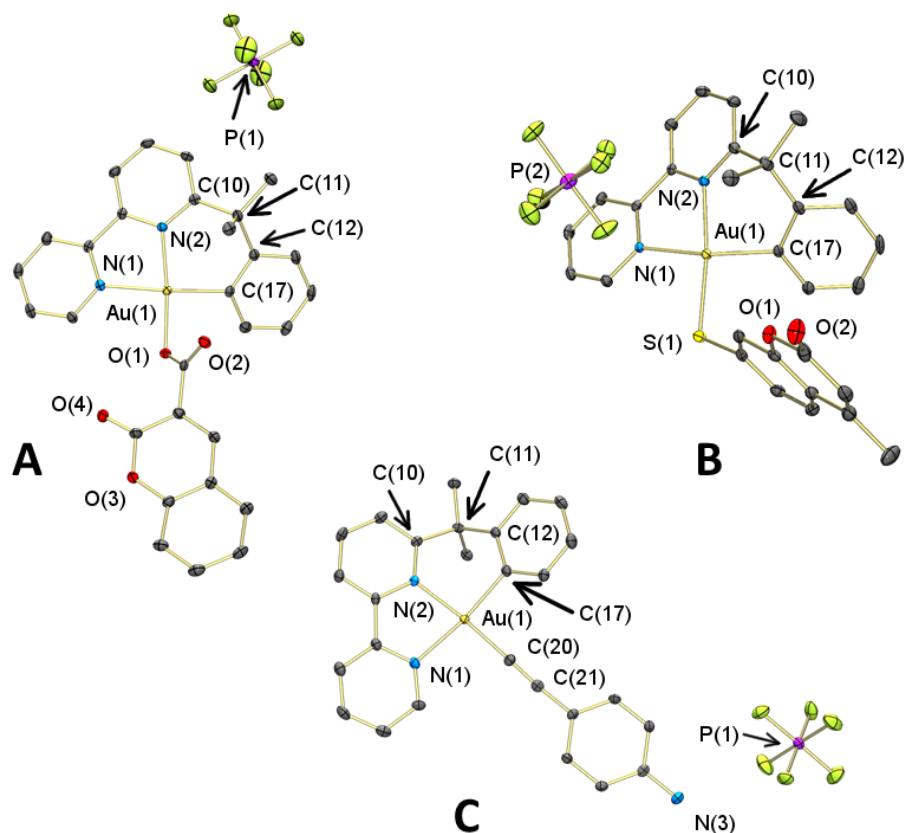


Figure 3. Molecular structures of **2-PF₆** (**A**), **3-PF₆** (**B**) and **6-PF₆** (**C**) with ellipsoids set at 30% probability level. Hydrogens were omitted for clarity. Also omitted in **A** is a second, partially occupied PF₆⁻; symmetry operation to generate equivalent atoms: $1-x, 1-y, 1-z$. In **B** a molecule of acetonitrile was omitted.

Analysis of packing interactions shows that **2-PF₆** forms a dimeric aggregate with a neighbouring unit *via* short O...H contacts between the carbonyl oxygen O(4) and hydrogen atom H(2) [O(4)...H(2)ⁱ 2.374 Å, $i = 1-x, -y, -z$] (Figure S17-18). The solid state structure develops further through π -stacking interactions between neighbouring phenyl rings of two cyclometalated ligands [mean plane distance C(12)-C(17)...C(12)ⁱⁱ-C(17)ⁱⁱ = 3.605(5) Å, $ii = 1-x, 1-y, 1-z$] (Figure S19); the rings are slightly slipped [centroid-centroid distance 3.998(4) Å] and parallel to each other [plane twist angle 0.0(8)°], with their interaction aided by an additional hydrogen contact which locks the conformation [O(2)...H(14)ⁱⁱ 2.374 Å, $ii = 1-x, 1-y, 1-z$] (Figure S18-19). Significant intermolecular long-range interactions are also present in **3-PF₆**, which displays a ladder-type arrangement. Such a conformation comprises four molecular units interlocked *via* π -stacking of two coumarins sandwiched between two phenyl rings of the cyclometalated ligand [mean plane distance coumarin-phenyl 3.672(2) Å; mean plane

distance coumarin-coumarin 3.506(3) Å, see Figure S20]; the coumarins are stacked in a similar fashion to what observed for complex (C[^]N[^]P^z^C)AuS-4-methylcoumarin [C[^]N[^]P^z^C = N₂C₄H₂ {Ph('Bu)}-2,6].⁵ Finally, complex **6**-PF₆ shows intermolecular π-stacking interactions between the pyridyl and aminopyridyl rings of two adjacent units [centroid-centroid distance N(1)-C(5)···C(22)-C(27)ⁱ 3.710(2), mean plane N(1)-C(5) to C(22)ⁱ 3.326(6) Å, *i* = 2-*x*, 1-*y*, 1-*z*, twist angle 5.83(17)°] (Figure S21). Additionally, the alkynyl unit C(20)≡C(21) displays a short contact with a neighbouring alkynyl fragment [alkynyl···alkynyl 3.527(7) Å], thus contributing to the stacked conformation of the complex in the solid state (Figure S22).

An ORTEP view of compound **10** with the atom labelling scheme is shown in Figure 4 and selected bond lengths and angles reported in the caption to the figure. Compound **10** displays a nearly linear geometry around the Au center [C1-Au1-P1 = 173.5(2)°], featuring an alkyne ligand [Au1-C1 = 1.999(5) Å; C1-C2 = 1.180(8) Å] and an ancillary triphenylphosphane ligand [Au1-P1 = 2.266(2) Å].

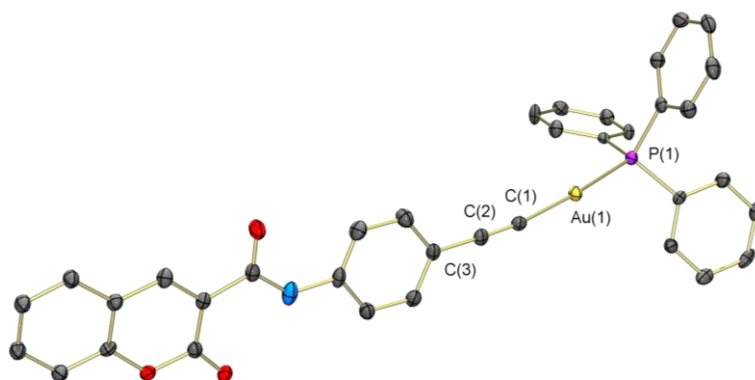


Figure 4. Molecular structure of compound **10** with ellipsoids set at 30% probability level. Hydrogens have been omitted for clarity. Selected bond lengths (Å) and angles (deg.): Au1-C1 1.999(5), Au1-P1 2.266(2), C1-C2 1.180(8); P1-Au-C1 173.5(2), Au1-C1-C2 170.7(5), C1-C2-C3 177.4(6).

Packing analysis shows no significant π-stacking interactions in the solid state structure, with the closest contact being between one the phenyl rings of the PPh₃ [C(31)-C(36)] fragment and the bridging phenyl linker of the alkynyl ligand, C(3)-C(8), [3.911(3) Å; twist angle 16.8(2)°].

Antiproliferative Properties

The antiproliferative properties were assessed by monitoring the ability of the investigated gold complexes to inhibit cell growth using the classical MTT assay as described in the Experimental section. Initially, the compounds were tested against human lung epithelial

cancer (A549) and human ovarian cancer (SKOV-3) cancer cells. Table S4 in the supplementary material summarizes the preliminary obtained EC₅₀ data of all complexes in these two cell lines. According to the obtained results, only complexes **3**-PF₆ and **5**-PF₆ display antiproliferative effects, with **5**-PF₆ being the most efficient, while all the others are scarcely or non-active in both cell lines. Of note, all the free ancillary ligands showed EC₅₀ values above 50 μM (data not shown). Moreover, the Au^I complex [Au(C₂ArNHCOQ)(PPh₃)] (**10**), featuring the same ancillary ligand as **5**-PF₆, showed very moderate effects in cancer cells (Table S4).

Thus, the most effective compounds **3**-PF₆ and **5**-PF₆ were evaluated in other cell lines, including human breast cancer (MCF-7), human melanoma (A375), and the non-tumorigenic human embryonic kidney (HEK-293) cells. The resulting EC₅₀ values are shown in Table 1 and compared to those of cisplatin and of the free ancillary ligand of complex **3**-PF₆, HC₂ArNHCOQ. In general, compound **3**-PF₆ behaves similarly to cisplatin in the A549 and SKOV-3 cell lines. Instead, **5**-PF₆ is a far better inhibitor of cell proliferation than cisplatin, leading to the hypothesis that the compound may be active *via* different mechanisms. Unfortunately, while **3**-PF₆ is scarcely toxic against the non-tumorigenic HEK-293 cells, **5**-PF₆ shows scarce selectivity.

It should be noted that the observed differences in antiproliferative effects may be due to various reasons, including the stability of the compounds in aqueous solution, as well as possible differences in their intracellular accumulation profiles. Previously reported studies have shown that this type of Au^{III} C^NN complexes - [Au(bipy^{dmb}-H)X]⁺ - possess high redox stability in aqueous solution while they tend to hydrolyse the ancillary X ligands to form [Au(bipy^{dmb}-H)(OH)]⁺.^{21,22} However, in order to further explore the differences among the biological properties of the compounds, we have studied the stability of the most active complexes **3**-PF₆ and **5**-PF₆ in comparison to the one of the least cytotoxic analogue **6**-PF₆ (see Table S4) by UV-visible spectrophotometry. Figure S23 shows the representative absorption spectra of the two complexes **5**-PF₆ and **6**-PF₆ recorded in PBS (pH 7.4) at different times over 24 h. As it can be observed, complex **5**-PF₆ is perfectly stable during time (Figure S23A), and similar results have been obtained for complex **3**-PF₆. Conversely, **6**-PF₆ undergoes marked spectral changes due to fast hydrolysis and possibly reduction of the gold(III) centre, as witnessed by the immediate disappearance of band centred at 320 nm, characteristic of the {Au^{III}(bipy^{dmb}-H)} scaffold (Figure S23B). The stability of **5**-PF₆ in the presence of the intracellular reducing agent glutathione (GSH) has also been studied by UV-Vis spectrophotometry (Figure S24), and the results shows that the compound is able to form adducts with GSH right after mixing the two components.

Table 1. EC₅₀ values determined after 72 h of exposure to the gold complexes **3**-PF₆ and **5**-PF₆ and the respective free ligands MeQS and HC₂ArCONHQ.

Compound	Effective Concentration (EC ₅₀ / μM) ^a				
	A549	MCF-7	SKOV-3	A375	HEK-293
3 -PF ₆	17.6 ± 2.4	-	15.1 ± 1.9	44.15 ± 12.30	54.38 ± 9.04
5 -PF ₆	4.5 ± 0.8	2.3 ± 0.8	2.6 ± 0.8	1.46 ± 1.07	0.55 ± 0.01
HC ₂ ArNHCOQ	>100	>100	>100	>100	>100
MeQS	>80	>80	>80	>80	>80
cisplatin	11.5 ± 0.9	20 ± 3	13 ± 4	3.10 ± 1.59	8.15 ± 0.47

^a Mean ± ES of three independent experiments performed with triplicate cultures at each tested concentration.

Mass spectrometry

Reaction with cytochrome c, cysteine and histidine

Investigating the stability and ligand exchange reactions of putative metallodrugs is important for implementing their further design. ESI MS is ideally suited for this purpose because the *m/z* information allows conclusions on the mechanisms of reactivity of metallodrugs at a molecular level.⁴²⁻⁴³ Thus, compounds **1OH**-PF₆, **5**-PF₆, **6**-PF₆ and **9**-PF₆ were incubated with the model protein cytochrome c (cyt c) at 3:1 metal-to-protein ratio for 24 h at 37 °C, and with the amino acids cysteine and histidine at different incubation time (10 min, 1, 3 and 24 h) at 1:1 metal-to-amino acid ratio. Of note, all the tested compounds did not form any adducts with the protein cyt c (data not shown). Intriguingly, the dinuclear oxo-bridged analogue³⁹ of **1OH**-PF₆ reacted with cyt c, as studied by high-resolution LTQ-Orbitrap ESI MS, by forming mono- and bis-adducts containing [Au^{III}(bipy^{dmb}-H)]²⁺ fragments.⁴⁴ Moreover, all the new Au^{III} compounds do not react with histidine but they form adduct with cysteine (Figure 5), made exception of **6**-PF₆ which results completely unreactive in the selected experimental conditions (data not shown). Formation of [Au(bipy^{dmb}-H)Cys]⁺ adduct begins after 1 h incubation and generally increases over time in all cases. This is in line with our previously reported ESI MS data on the reactivity of the hydroxo precursor [Au(bipy^{dmb}-H)(OH)][PF₆] **1OH**-PF₆,⁴⁵ forming predominantly monomeric Au^{III} adducts. A summary of the obtained data for the investigated compounds reacting with Cys after 24 h incubation is provided in Table 2 and Figure 5. The lack of reactivity of **6**-PF₆ with biomolecules, together with its pronounced instability, may also be responsible for its scarce cytotoxicity against cancer cells.

Table 2. Experimental (*m*_{exp}) and theoretical (*m*_{theor}) mass signals attributed to each specie during ESI-QTOF MS experiments of compounds **1OH**-PF₆, **5**-PF₆ and **9**-PF₆ reacting with Cys after 24 h incubation. All experimental mass signals include a standard deviation of *m/z* of 0.05.

Compound	Species	<i>m</i> _{exp}	<i>m</i> _{theor}
1OH -PF ₆	[Au(bipy ^{dmb} -H)OH] ⁺	487.16	487.11
	[Au(bipy ^{dmb} -H)Cys] ⁺	590.16	590.12

5 -PF ₆	[Au(bipy ^{dmb} -H)OH] ⁺	487.16	487.11
	[Au(bipy ^{dmb} -H)Cys] ⁺	590.16	590.12
	[Au(bipy ^{dmb} -H)(C ₂ ArNHCOQ)] ⁺	758.22	758.17
9 -PF ₆	[Au(bipy ^{dmb} -H)Cys] ⁺	590.18	590.12
	[Au(bipy ^{dmb} -H)GS] ⁺	776.26	776.18

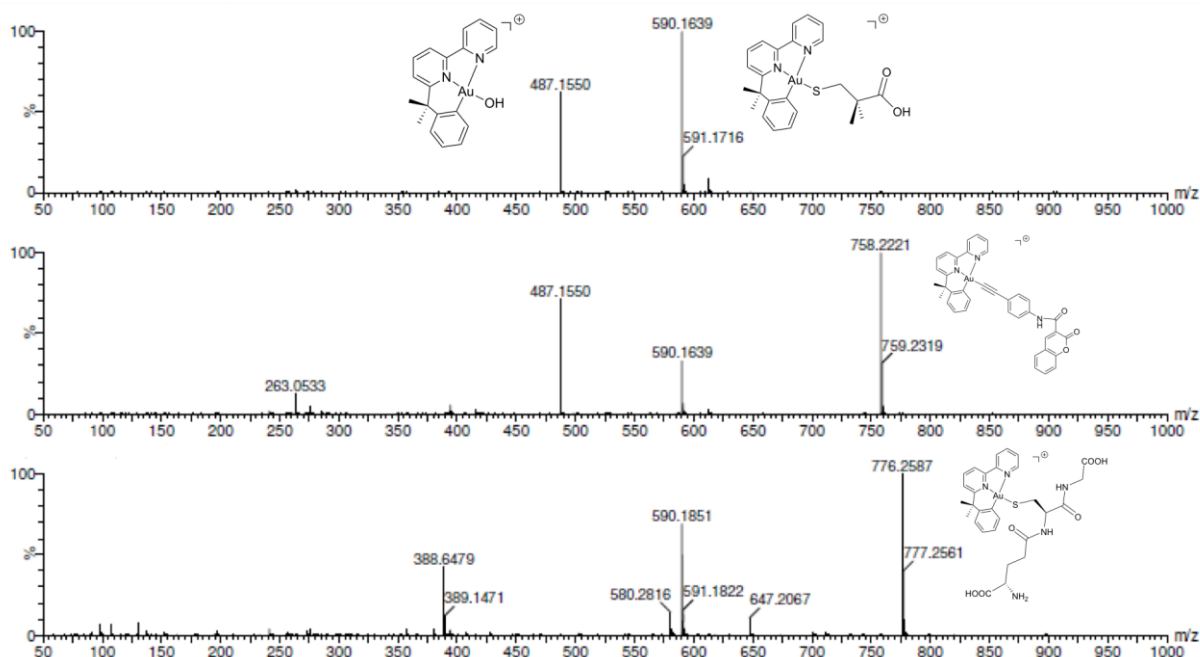


Figure 5. Representative ESI-MS spectra and peak assignments of complexes **10H**-PF₆, **5**-PF₆ and **9**-PF₆ with cysteine (1:1, 150 μM) after 24 h incubation.

Competitive Reaction with ubiquitin and model DNA

Capillary zone electrophoresis (CZE)–ESI MS turned out to be ideally suited to investigate the binding preferences of metallo(-pro)drugs towards mixtures of protein and DNA under competitive conditions.^{35,46} CZE separates analytes according to charge and size and is thus ideally suited to separate hydrolysis products of metallo(-pro)drugs as well as potential adducts with biomolecules. Therefore, ubiquitin (ub), a widely used model peptide for interaction studies featuring a N-terminal methionine residue and a histidine,⁴³ and a single strand oligonucleotide (5′-dATTGGCAC-3′) were mixed in aqueous solution with **10H**-PF₆ in a 1:1:4 molar ratio, incubated at 37 °C and reaction aliquots were analyzed after 10 min, 1 h and 6 h (see Experimental for details). Under these conditions, and already after 10 min incubation, a large portion of the DNA has reacted with the gold compound producing [DNA + n{Au(bipy^{dmb}-H)}] (n = 1-4) adducts, while adducts with ub were not observed (Table 3). The unreacted cation of **10H**-PF₆ was found at all three incubation time points with

the highest intensities at 10 min (Figure 6). All the analytes were baseline-separated in time by CZE. After 10 min the bis-adduct gave the highest product signal intensities, whereas after 6 h the tris-adduct showed the most intense peak. Thus, the DNA oligomer seems to feature three stable binding sites on the nucleotides, which are kinetically favored over amino acid binding. Overall, these results show the pronounced reactivity of the compound with oligonucleotides with respect to peptides and amino acids.

Table 3. List of experimental (m_{exp}) and theoretical (m_{theor}) mass signals attributed to each species observed in CZE–ESI-MS experiments for **1OH**-PF₆. The accuracy of the mass signals is expressed as the deviation in parts per million (Δppm).

Species	m_{exp}	m_{theor}	Δppm
[1OH] ⁺	487.1111	487.1079	6.6
[Au(bipy ^{dmb} -H)(COOH)] ⁺	515.1051	515.1028	4.5
[ub + 9H] ⁹⁺	952.6383	952.6329	5.7
[DNA + 4{Au(bipy ^{dmb} -H)} - 3H] ⁵⁺	857.3735	857.3698	4.3
[DNA + 3{Au(bipy ^{dmb} -H)} - 2H] ⁴⁺	954.4416	954.4379	3.9
[DNA + 2{Au(bipy ^{dmb} -H)}] ⁴⁺	837.4201	837.4153	5.7
[DNA + Au(bipy ^{dmb} -H) + H] ³⁺	960.1909	960.1880	3.0
[DNA + 3H] ³⁺	803.8268	803.8237	3.9

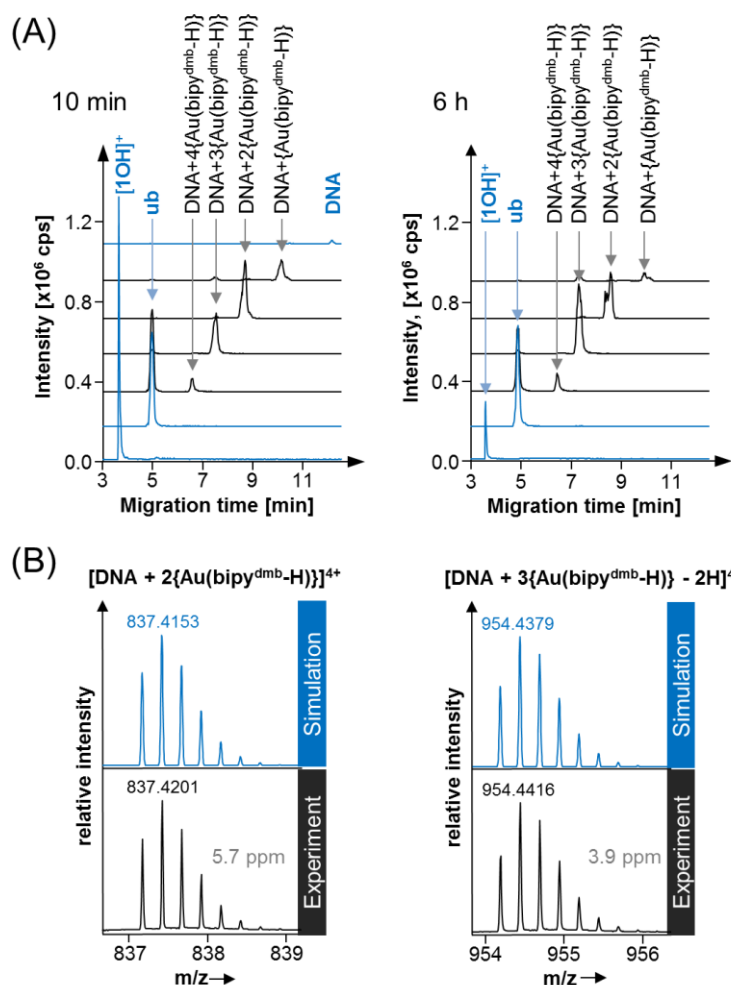


Figure 6. (A) Representative extracted-ion-electropherograms (EIEs) of **10H**-PF₆ incubated with ubiquitin (ub) and the oligonucleotide 5'- dATTGGCAC-3' (DNA) for 10 mins and 6 h. (B) Experimental and simulated mass spectra of the most intense [**10H**]-DNA adducts obtained by CZE-ESI-MS.

Conclusions

The synthesis of a new series of (C^NN) cyclometalated Au^{III} complexes featuring the 6-(1,1-dimethylbenzyl)-2,2'-bipyridine) scaffold has been reported and the compounds have been characterized *via* different methods, including some by X-ray diffraction. All the complexes were studied for their absorption and photophysical properties, showing typical IL and MLCT absorption bands in the UV-Vis region, while they feature a main emission band centred around 350 nm which is largely attributable to the bipy^{dmb} ligand. Unfortunately, the photoactive ancillary ligands quench their fluorescence upon binding to the Au^{III} centre, most likely due to an ISC relaxation path favoured by the gold metal ion.

The compounds were evaluated for their antiproliferative properties *in vitro* and their activity was shown to be highly dependent on the nature of the ancillary ligand. Specifically, both Au^{III} complexes **3**-PF₆ and **5**-PF₆, featuring coumarin ligands, showed the most

pronounced anticancer activity, although **5**-PF₆ displayed scarce selectivity towards cancer cells with respect to non-tumorigenic ones. In the future, the selectivity of the compound may be improved tethering it to targeting peptides *via* derivatization of the cyclometalated scaffold. The stability of representative complexes (**3**-PF₆, **5**-PF₆ and **6**-PF₆) in aqueous environment has been studied by UV-Vis spectrophotometry, showing that the least cytotoxic complex **6**-PF₆ is also very unstable in solution. Moreover, the reactivity of selected Au^{III} C^NN complexes was evaluated with model biomolecules by MS approaches and the results strongly point toward a preferred binding affinity for nucleic acid structures with respect to proteins, at variance with what has been observed so far for other types of cyclometalated Au^{III} compounds (e.g. of the C^N type). Due to the fact that only two Au^{III} derivatives out of eleven compounds tested showed appreciable antiproliferative activity, it is difficult to draw meaningful structure-activity relationships. However, it can be hypothesized that several factors can be responsible for the scarce anticancer effects displayed by the majority of the Au^{III} complexes: *i*) scarce reactivity with biomolecules, *ii*) reduced stability in aqueous environment, and *iii*) scarce cell uptake/accumulation. Thus, although these preliminary results may constitute the basis for the design of organogold compounds targeted to nucleic acid structures, further studies are necessary to gain mechanistic insights. Overall, while some of the compounds display promising anticancer activities and the selected scaffolds constitute attractive leads for further drug design, the quest for selectivity of such complexes toward cancer cells still needs to be addressed.

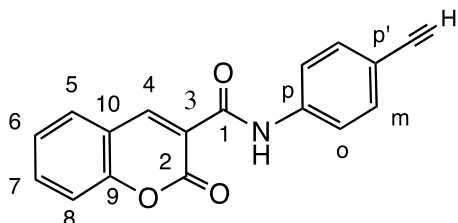
Experimental section

General. All reactions were carried out under air and solvents were dried and distilled before use. The precursors [Au(bipy^{dmb}-H)Cl][PF₆] (**1Cl**-PF₆), [Au(bipy^{dmb}-H)(OH)][PF₆] (**1OH**-PF₆), [Au(bipy^{dmb}-H)(OMe)][PF₆] (**1OMe**-PF₆), [Au(bipy^{dmb}-H)(CH₂COCH₃)][PF₆] (**1CH₂Ac**-PF₆) were synthesized according to procedures reported in refs.³⁶⁻³⁸ The analytical data obtained for these four complexes were in agreement with published data. All other reagents and ligands, with the exception of HC₂ArNHCOQ, were purchased from the Sigma-Aldrich. Infrared spectra were recorded with a Jasco FTIR 480 Plus spectrophotometer using Nujol mulls. UV-Vis spectra were recorded on a Varian Cary 50 or on a Hitachi U-2010 UV-Vis Thermo Nicolet Evolution 300 (190–1100 nm) spectrophotometer at room temperature using quartz cuvettes with an optical path length of 10.0 mm; spectra were recorded on MeCN solutions. Emission and excitation spectra were obtained at room temperature with a Varian Cary Eclipse Fluorescence spectrophotometer (Xe lamp) using quartz cuvettes with an optical path length of 10.0 mm. Absorption and emission electronic spectra were recorded on MeCN and CH₂Cl₂

solutions. ^1H , ^{13}C , and ^{31}P NMR spectra were recorded at room temperature (20 °C) on a Bruker Avance III 400 spectrometer operating at 400.0, 100.5 and 161.8 MHz, respectively. Chemical shifts are given in ppm relatively to internal TMS (^1H), and external H_3PO_4 (^{31}P).

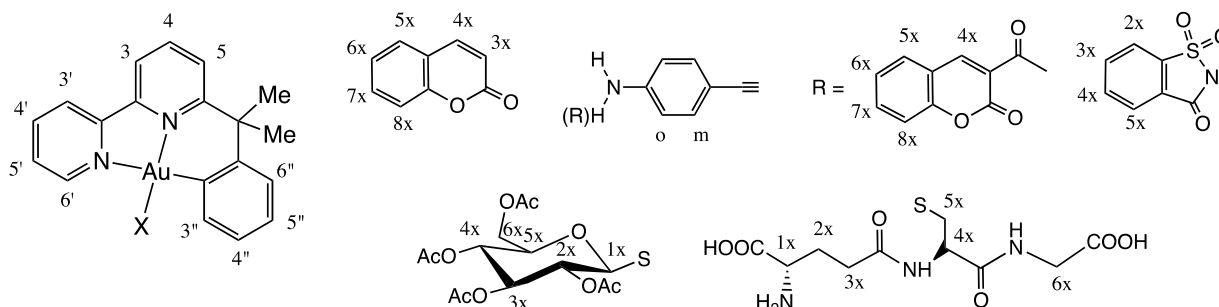
Syntheses

Synthesis of the ligand $\text{HC}_2\text{ArNHCOQ}$.



To a stirred solution of QCO_2H (0.500 g, 2.6 mmol) in dichloromethane (5 mL) were added the coupling agent *N*-(3-dimethylaminopropyl)-*N'*-ethylcarbodiimide (EDC) (0.419 g, 2.7 mmol, $d = 0.877 \text{ g/mL}$) and a dichloromethane solution (2 mL) of HC_2ArNH_2 (0.340 g, 2.9 mmol) at room temperature. The reaction mixture was then cooled to 0°C and stirred for 24 h. The resulting yellow solid was filtered under vacuum and washed with water, ethanol and diethyl ether (58% yield). ^1H NMR (CDCl_3); assignments based on COSY and NOESY experiments: δ 3.05 (s, 1H; HC_2), 7.41 (t, part. overlapped, 1H, $J = 7.2 \text{ Hz}$; H^6), 7.44 (d, part. overlapped, 1H, $J = 8.8 \text{ Hz}$; H^8), 7.49 (d, 2H, $J = 8.0 \text{ Hz}$; H^m), 7.70 (t, part. overlapped, 1H, $J = 8.0 \text{ Hz}$; H^7), 7.71 (d, 2H, $J = 8.8 \text{ Hz}$; H^o), 7.72 (d, part. overlapped, 1H, H^5), 9.00 (s, 1H; H^4), 10.92 (s, 1H; NH). ^{13}C NMR (CDCl_3): δ 77.4 ($\text{C}\equiv\text{CH}$), 83.6 ($\text{C}\equiv\text{CH}$), 117.0 (C^8), 118.4, 118.6, 118.9 (C^3 , C^9 , $\text{C}^{p'}$), 120.4 (C^o), 125.8 (C^6), 130.2 (C^5), 133.2 (C^m), 134.8 (C^7), 138.3 (C^p), 149.4 (C^4), 154.7 (C^9), 159.6 (C^2), 162.0 (C^1). Selected IR bands ($\nu_{\text{max}} \text{ cm}^{-1}$): 3270 $\nu(\text{NH})$, 1702 $\nu(\text{C}=\text{O})$. UV-vis [CH_3CN , $\lambda_{\text{max}}/\text{nm}$ ($\epsilon/\text{M}^{-1}\text{cm}^{-1}$): 261 (13002), 304 (14747), 336 (16206).

Syntheses of the cyclometallated gold(III) complexes based on bipy^{dmb}



[Au($\text{bipy}^{\text{dmb}}\text{-H})(\text{QCO}_2)]][\text{PF}_6]$ (2-PF₆**). To a stirred solution of **1OH-PF₆** (0.0632 g, 0.1 mmol) in dichloromethane (5 mL) was added QCO_2H (0.019 g, 0.1 mmol). The reaction mixture was stirred at room temperature for 3 h. A white solid which formed was filtered under vacuum and**

recrystallized from dichloromethane/diethyl ether to give the analytical sample. Yield 83%; mp 220 °C. Anal. Calcd for C₂₉H₂₂AuF₆N₂O₄P: C, 43.30; H, 2.76; N, 3.48%. Found: C, 43.18; H, 2.60; N, 3.39%. ¹H NMR (CD₃CN): δ 2.14 (s, 6H; CH₃), 7.18 (td, 1H, *J* = 7.6, 1.6 Hz; H^{4''}), 7.37 (td, 1H, *J* = 7.6, 1.2 Hz; H^{5''}), 7.42 (t, part. overlapped, 1H, *J* = 7.6 Hz; H^{6x}), 7.43 (d, 1H, *J* = 7.6 Hz; H^{8x}), 7.51 (dd, 1H, *J* = 8.0, 1.6 Hz; H^{6''}), 7.66 (dd, 1H, *J* = 8.0, 1.2 Hz; H^{3''}), 7.73 (td, 1H, *J* = 8.0, 1.6 Hz; H^{7x}), 7.79 (dd, 1H, *J* = 8.0, 1.2 Hz; H^{5x}), 8.02 (ddd, 1H, *J* = 7.6, 5.6, 1.2 Hz; H⁵), 8.21 (dd, 1H, *J* = 6.4, 2.8 Hz; H⁵), 8.47-8.52 (m, 3H; H³ + H⁴ + H⁴), 8.60 (d, 1H, *J* = 8.0 Hz; H^{3'}), 8.64 (s, 1H; H^{4x}), 9.02 (dd, 1H, *J* = 5.6, 1.2 Hz; H^{6'}). Selected IR bands (*v*_{max} cm⁻¹): 1728 *v*(C=O), 1708 *v*(CO₂ asym), 1608, 1322 *v*(CO₂ sym), 842 *v*(PF₆). UV-vis [CH₃CN, λ_{max}/nm (ε/M⁻¹cm⁻¹): 299 (18471), 255 (sh, 12900), 305 (17300), 326 (17900). Emission spectrum, (λ_{em} nm) = 410. X-ray quality crystals of **2**-PF₆ were obtained by slow diffusion of diethyl ether into a concentrate dichloromethane solution.

[Au(bipy^{dmb}-H)(MeQS)][PF₆] (3-PF₆). To a stirred solution of **1OH**-PF₆ (0.0632 g, 0.1 mmol) in dichloromethane (5 mL) was added solid MeQSH (0.019 g, 0.1 mmol). The resulting reaction mixture was stirred at room temperature for 24h. An orange solid which formed was filtered under vacuum and recrystallized from dichloromethane/diethyl ether to give the analytical sample. Yield 88%; mp 230 °C (dec). Anal. Calcd for C₂₉H₂₄AuF₆N₂O₂PS: C, 43.19; H, 3.00; N, 3.47%. Found: C, 43.05; H, 2.97; N, 3.41%. ¹H NMR (CD₃CN); assignments based on COSY and NOESY experiments: δ 2.06 (s, 6H; CH₃), 2.35 (d, 3H, *J* = 1.2 Hz; CH₃), 6.20 (d, 1H, *J* = 1.2 Hz; H^{3x}), 7.08 (td, 1H, *J* = 7.6, 1.2 Hz; H^{4''}), 7.27 (ddd, 1H, *J* = 7.8, 7.4, 1.2 Hz; H^{5''}), 7.48 (d, part. overlapped, 1H, *J* = 8.4 Hz; H^{5x}), 7.49 (dd, part. overlapped, 1H, *J* = 8.0, 1.6 Hz; H^{6''}), 7.56 (dd, 1H, *J* = 8.4, 2.0 Hz; H^{6x}), 7.60 (d, 1H, *J* = 2.0 Hz; H^{8x}), 7.95 (ddd, 1H, *J* = 7.6, 5.6, 1.2 Hz; H⁵), 8.09 (dd, 1H, *J* = 7.6, 1.2 Hz; H^{3''}), 8.16 (dd, 1H, *J* = 8.0, 1.2 Hz; H⁵), 8.44 (t, part. overlapped, 1H, *J* = 8.0 Hz; H⁴), 8.46 (td, part. overlapped, 1H, *J* = 8.4, 1.6 Hz, H^{4'}), 8.50 (dd, 1H, *J* = 8.0, 0.8 Hz; H³), 8.58 (d, 1H, *J* = 8.0 Hz; H^{3'}), 9.32 (dd, 1H, *J* = 5.6, 1.2 Hz; H^{6'}). Selected IR bands (*v*_{max} cm⁻¹): 1719 *v*(C=O), 1596 *v*(C=C) + *v*(C=N), 842 *v*(PF₆). UV-vis [CH₃CN, λ_{max}/nm (ε/M⁻¹cm⁻¹): = 292 (17800), 306 (21000), 334 (21700). Emission spectrum, (λ_{em} nm) = 374. X-ray quality crystals of **3**-PF₆ were obtained by slow diffusion of diethyl ether into a concentrate acetonitrile solution.

[Au(bipy^{dmb}-H)(CF₃QNH)][PF₆] (4-PF₆). *Method A*: To a stirred solution of **1OH**-PF₆ (0.0632 g, 0.1 mmol) in toluene (5 mL) was added solid CF₃QNH₂ (0.0229 g, 0.1 mmol). The reaction mixture was stirred at room temperature for 24h. A red solid which formed was filtered under vacuum and washed with Et₂O. Recrystallization from dichloromethane/diethyl ether gave the analytical sample (29% yield). *Method B*: To a stirred solution of **1OMe**-PF₆ (0.0646 g, 0.1 mmol) in dichloromethane (10 mL) was added solid CF₃QNH₂ (0.0687 g, 0.3 mmol). The reaction mixture was stirred at room temperature for 24h. A red solid which formed was filtered under vacuum and recrystallized from dichloromethane/diethyl ether to give the analytical

sample. Yield 50%; mp 230 °C (dec). Anal. Calcd for C₂₉H₂₂AuF₉N₃O₂P: C, 41.30; H, 2.63; N, 4.98%. Found: C, 41.35; H, 2.57; N, 5.03%. ¹H NMR (CD₂Cl₂): δ 2.20 (s, 6H; CH₃), 5.49 (s, 1H, NH), 6.44 (s, 1H; H^{3x}), 6.80 (s, 1H; H^{8x}), 6.93 (d, 1H, *J* = 8.8 Hz; H^{6x}), 7.11 (t, 1H, *J* = 7.6 Hz; H^{4''}), 7.35 (t, 1H, *J* = 7.4 Hz; H^{5''}), 7.44 (d, 1H, *J* = 8.0 Hz; H^{6''}), 7.48 (d, 1H, *J* = 8.8 Hz; H^{5x}), 7.55 (d, 1H, *J* = 8.0 Hz; H^{3''}), 7.99 (t, 1H, *J* = 6.8 Hz; H^{5'}), 8.17 (d, 1H, *J* = 7.6 Hz; H⁵), 8.52 (t, 1H, *J* = 7.4 Hz; H⁴), 8.54 (d, 1H, *J* = 7.6 Hz; H³), 8.55 (t, 1H, *J* = 8.0 Hz; H^{4'}), 8.65 (d, 1H, *J* = 8.4 Hz; H^{3'}), 9.06 (d, 1H, *J* = 5.6 Hz; H^{6'}). Selected IR bands (ν_{max} cm⁻¹): 1721 ν(C=O), 1598 ν(C=C) + ν(C=N), 843 ν(PF₆). UV-Vis [CH₃CN, λ_{max}/nm (ε/M⁻¹cm⁻¹): 248 (22600), 325 (13300), 411 (11900). Emission spectrum, (λ_{em} nm) = 462.

[Au(bipy^{dmb}-H)(C₂ArNHCOQ)][PF₆] (5-PF₆). *Method A.* To a stirred solution of **1OH**-PF₆ (0.0632 g, 0.1 mmol) in toluene (5 mL) was added solid HC₂ArNHCOQ (0.0289 g, 0.1 mmol), 1:1. The reaction mixture was refluxed at 80°C for 24h. A yellow solid which formed was filtered under vacuum, washed with Et₂O and recrystallized from dichloromethane/diethyl ether to give the analytical sample (33% yield). *Method B.* To a stirred solution of **1OMe**-PF₆ (0.0646 g, 0.1 mmol) in toluene (10 mL) was added solid HC₂ArNHCOQ (0.0868 g, 0.3 mmol); a small amount of dichloromethane was then added until a solution was obtained. The reaction mixture was stirred at room temperature for 24h. The resulting solution was evaporated to dryness and the yellow residue recrystallized from dichloromethane/diethyl ether to give the analytical sample. Yield 61%. *Method C.* To a stirred solution of **1CH₂Ac**-PF₆ (0.0672 g, 0.1 mmol) in toluene (5 mL) was added solid HC₂ArNHCOQ (0.0289 g, 0.1 mmol). The reaction mixture was refluxed at 80°C for 48h. A yellow solid which formed was filtered under vacuum and washed with Et₂O; recrystallization from dichloromethane/diethyl ether gave the analytical sample. Yield 46%; mp 220 °C (dec). Anal. Calcd for C₃₇H₂₇AuF₆N₃O₃P: C, 49.18; H, 3.01; N, 4.65%. Found: C, 49.20; H, 2.97; N, 4.61%. ¹H NMR (CD₂Cl₂): δ 2.16 (s, 6H; CH₃), 7.24 (t, 1H, *J* = 7.4 Hz; H^{4''}), 7.43 (t, 1H, *J* = 7.6 Hz; H^{5''}), 7.49 (d, 1H, *J* = 8.0 Hz; H^{6''}), 7.51 (m, 2H; H^{6x} + H^{8x}), 7.58 (d, 1H, *J* = 8.0 Hz; H^{3''}), 7.67 (d, 2H, *J* = 8.0 Hz; H^m), 7.79 (t, 1H, *J* = 8.0 Hz; H^{7x}), 7.86 (d, broad, 3H, *J* = 7.2 Hz; H^{5x} + H^o), 8.07 (t, 1H, *J* = 6.2 Hz; H^{5'}), 8.19 (d, 1H, *J* = 7.2 Hz; H⁵), 8.29 (d, 1H, *J* = 8.0 Hz; H³), 8.54 (t, 1H, *J* = 8.0 Hz; H^{4'}), 8.56 (t, 1H, *J* = 8.0 Hz; H⁴), 8.68 (d, 1H, *J* = 8.0 Hz; H^{3'}), 9.08 (s, 1H; H^{4x}), 9.53 (d, 1H, *J* = 5.2 Hz; H^{6'}), 11.03 (s, 1H, NH). Selected IR bands (ν_{max} cm⁻¹): 3268 ν(NH), 1716 ν(C=O), 1609 ν(C=C) + ν(C=N), 837 ν(PF₆). UV-Vis [CH₃CN, λ_{max}/nm (ε/M⁻¹cm⁻¹): 262 (29100), 331 (32300). Emission spectrum (λ_{em} nm) = 365.

[Au(bipy^{dmb}-H)(C₂ArNH₂)](PF₆) (6-PF₆). To a stirred solution of **1Cl**-PF₆ (0.0651 g, 0.1 mmol) in ethanol (5 mL) were added solid HC₂ArNH₂ (0.0117 g, 0.1 mmol) and an ethanol solution of tBuOK (0.0224 g, 0.2 mmol). The reaction mixture was stirred at room temperature for 24h. The resulting solution was evaporated to dryness and the orange solid recrystallized from dichloromethane/diethyl ether to give the analytical sample. Yield 45%; mp 210 (dec). Anal.

Calcd for $C_{27}H_{23}AuF_6N_3P$: C, 44.34; H, 3.17; N, 5.74%. Found: C, 44.30; H, 3.12; N, 5.69%. 1H NMR (CD_3CN): δ 2.04 (s, 6H; CH_3), 4.46 (s, 2H; NH_2), 6.65 (dt, 2H, $J = 8.4, 2.1$ Hz; H^o), 7.17 (td, 1H, $J = 8.0, 1.6$ Hz; $H^{4''}$), 7.36 (dt, part. overlapped., 2H, $J = 8.4, 2.0$ Hz; H^m), 7.37 (td, 1H, $J = 6.8, 1.2$ Hz; $H^{5''}$), 7.57 (dd, 1H, $J = 8.0, 1.6$ Hz; $H^{6''}$), 8.03 (ddd, 1H, $J = 7.6, 5.6, 1.2$ Hz; $H^{5''}$), 8.16 (dd, 1H, $J = 7.2, 1.6$ Hz; $H^{3''}$), 8.22 (dd, 1H, $J = 8.0, 1.2$ Hz; H^5), 8.43 (t, 1H, $J = 8.0$ Hz; H^4), 8.44 (d, 1H, $J = 7.2$ Hz; H^3), 8.47 (td, 1H, $J = 8.0, 1.2$ Hz; $H^{4''}$), 8.56 (d, 1H, $J = 8.0$ Hz; $H^{3''}$), 9.44 (dd, 1H, $J = 5.4, 1.2$ Hz; $H^{6''}$). Selected IR bands (ν_{max} cm^{-1}): 3393 $\nu(NH)$, 2159 $\nu(C\equiv C)$, 1623, 1605 $\nu(C=C) + \nu(C=N)$, 841 $\nu(PF_6)$. UV-Vis [CH_3CN , λ_{max}/nm ($\epsilon/M^{-1}cm^{-1}$): 277 (25922), 279 (27100), 316sh (16000), 400 (2200). Emission spectrum, (λ_{em} nm) = 351.

[Au(bipy^{dmb}-H)(Sacc)][PF₆] (7-PF₆). To a stirred suspension of **1Cl**-PF₆ (0.0651 g, 0.1 mmol) in water (5 mL) was added an aqueous solution SaccNa (0.021 g, 0.1 mmol). The reaction mixture was left at room temperature for 24h. The resulting suspension was filtered under vacuum and washed with ethanol and diethyl ether and the white solid recrystallized from acetone/diethyl ether to give the analytical sample. Yield 71%; mp 255 °C. Anal. Calcd for $C_{26}H_{21}AuF_6N_3O_3PS$: C, 39.16; H, 2.65; N, 5.27%. Found: C, 39.15; H, 2.67; N, 5.31%. 1H NMR (acetone-*d*₆): δ 2.28 (s, 6H; CH_3), 7.06 (t, 1H, $J = 7.4$ Hz; $H^{4''}$), 7.36 (t, 1H, $J = 7.4$ Hz; $H^{5''}$), 7.50 (d, 1H, $J = 8.0$ Hz; $H^{6''}$), 7.58 (d, 1H, $J = 7.2$ Hz; $H^{3''}$), 8.01-8.11 (m, 4H; $H^{2x} + H^{3x} + H^{4x} + H^{5''}$), 8.16 (d, 1H, $J = 7.2$ Hz; H^{5x}), 8.46 (d, 1H, $J = 8.0$ Hz; H^5), 8.70 (t, 1H, $J = 8.0$ Hz; H^4), 8.78 (t, 1H, $J = 8.0$ Hz; $H^{4''}$), 8.95 (d, 1H, $J = 8.0$ Hz; H^3), 9.03 (d, 1H, $J = 8.0$ Hz; $H^{3''}$), 9.09 (d, 1H, $J = 5.2$ Hz; $H^{6''}$). IR in Nujol (ν_{max} cm^{-1}): 1697 $\nu(C=O)$, 1602 $\nu(C=C) + \nu(C=N)$, 1176 $\nu(SO_2)$, 845 $\nu(PF_6)$. UV-Vis [CH_3CN , λ_{max}/nm ($\epsilon/M^{-1}cm^{-1}$): 253sh (14900), 329 (9800); Emission spectrum, (λ_{em} nm) = 462.

[Au(bipy^{dmb}-H)(GluS)][PF₆] (8-PF₆). To a stirred solution of **1OH**-PF₆ (0.0632 g, 0.1 mmol) in dichloromethane (5 mL) was added a solution of GluSH (0.0364 g, 0.1 mmol) in the same solvent. The reaction mixture was stirred at room temperature for 24h. the resulting light yellow solution was concentrated to a small volume and diethyl ether added to give a light yellow solid which was filtered under vacuum to give the analytical sample as a 1:0.2 mixture of two diastereomers (1H NMR criterium). Yield 82%; mp 175 °C. Anal. Calcd for $C_{33}H_{36}AuF_6N_2O_9PS$: C, 40.50; H, 3.71; N, 2.86%. Found: C, 40.39; H, 3.66; N, 2.78%. 1H NMR ($CDCl_3$): major species δ 1.90 (s, 3H; CH_3), 1.95 (s, 3H; CH_3), 1.97 (s, 3H; CH_3), 2.03 (s, 3H, CH_3), 2.10 (s, 6H; CH_3), 3.57 (d, broad, unresolved X part of an ABX spin system, 1H, $J = 9.2$ Hz; H^{5x}), 3.95 (dd, A part of an ABX spin system, 1H, $J_{AB} = 12.4$ Hz; $J_{AX} = 2.2$ Hz; $CH^A H^B$), 4.05 (dd, B part of an ABX spin system, 1H, $J_{AB} = 12.4$ Hz, $J_{BX} = 4.4$ Hz; $CH^A H^B$), 4.89 (d, 1H, $J = 9.6$ Hz; H^{1x}), 5.04 – 5.12 (m, 3H, $H^{2x} + H^{3x} + H^{4x}$), 7.12 (t, 1H+0.2H, $J = 8.0$ Hz; $H^{4''}$), 7.32 (t, 1H+0.2H, $J = 7.8$ Hz; $H^{5''}$), 7.46 (d, 1H, $J = 7.6$ Hz; $H^{6''}$), 7.90 (t, 1H, $J = 6.6$ Hz; H^5), 8.0 (d, 1H, $J = 8.0$ Hz, $H^{3''} / H^5$), 8.08 (d, 1H, $J = 8.0$ Hz; $H^5 / H^{3''}$), 8.43 (t, 2H, $J = 7.6$ Hz; $H^{4''} + H^4$), 8.64 (d, 1H, $J = 8.0$ Hz; H^3), 8.70 (d, 1H, $J = 8.0$ Hz; $H^{3''}$), 9.42 (d, 1H, $J = 4.8$ Hz; $H^{6''}$); minor species δ 1.98 (s,

part. overlapped, CH₃), 2.01 (s, 0.6H; CH₃), 2.08 (s, 0.6H; CH₃), 2.12 (s, 1.2H; CH₃), 3.77 (ddd, 0.2H, $J = 10.2, 4.4, 2.4$ Hz; H^{5x}), 4.20 (dd, A part of an ABX spin system, 0.2H, $J_{AB} = 12.6$ Hz, $J_{AX} = 2.0$ Hz; CH^AH^B), 4.30 (dd, B part of an ABX spin system, 0.2H, $J_{AB} = 12.6$ Hz, $J_{BX} = 4.4$ Hz; CH^AH^B), 4.63 (d, 0.2H, $J = 10.0$ Hz; H^{1x}), 5.15 – 5.28 (m, 0.6H; H^{2x} + H^{3x} + H^{4x}), 7.38 (d, 0.2H, $J = 7.6$ Hz; H^{6''}), 7.82 (d, 0.2H, $J = 8.4$ Hz; H^{3''} / H⁵), 7.97 (t, 0.2H, $J = 7.6$ Hz; H⁵), 8.12 (d, 0.2H, $J = 8.4$ Hz; H⁵/H^{3''}), 8.50 (t, 0.4H, $J = 8.0$ Hz; H⁴+H⁴), 8.68 (d, part. overlapped, 0.2H, $J = 7.6$ Hz; H³), 8.75 (d, 0.2H, $J = 8.0$ Hz; H³), 9.27 (d, 0.2H, $J = 4.8$ Hz; H⁶). Selected IR bands (ν_{\max} cm⁻¹): 1752 ν (CO₂ asym), 1600 ν (C=C) + ν (C=N), 1226 ν (CO₂ sym), 842 ν (PF₆). UV-Vis [CH₃CN, λ_{\max} /nm (ϵ /M⁻¹cm⁻¹): 256sh (18500), 322 (8700), 397 (370). Emission spectrum, (λ_{em} nm) = 359.

[Au(bipy^{dmb}-H)(GS)][PF₆] (9-PF₆). To a stirred solution of **10H**-PF₆ (0.0632 g, 0.1 mmol) in water (5 mL) was added an aqueous solution of GSH (0.0307 g, 0.1 mmol). The reaction mixture was stirred at room temperature for 24h. A light yellow solid which formed was filtered under vacuum and recrystallized from methanol/diethyl ether to give the analytical sample as a 1:0.1 mixture of two species, likely bond isomers. Yield 65%; mp 180 °C (dec). Anal. Calcd for C₂₉H₃₃AuF₆N₅O₆PS: C, 37.79; H, 3.61; N, 7.60%. Found: C, 37.76; H, 3.65; N, 7.57%. ¹H NMR (D₂O): major species δ 1.95 (s, 6H; CH₃), 1.99 (m, broad, 2H; CH₂-2x), 2.43 (dt, 2H, $J = 7.6$ Hz; CH₂-3x), 2.96 (dd, A part of an ABX spin system, 1H, $J_{AB} = 13.4$ Hz, $J_{AX} = 9.4$ Hz; CH^AH^B-5x), 3.30 (dd, B part of an ABX spin system, 1H, $J_{AB} = 13.4$ Hz, $J_{BX} = 4.6$ Hz; CH^AH^B-5x), 3.69 (t, 1H, $J = 6.4$ Hz, H^{1x}), 3.77 (s, 2H; H^{6x}), 4.44 (pseudo t, 1H, $J = 6.8, 6.0$ Hz; H^{4x}), 7.03 (t, 1H, $J = 7.4$ Hz; H^{4''}), 7.16 (t, 1H, $J = 7.4$ Hz; H^{5''}), 7.42 (d, 1H, $J = 7.6$ Hz; H^{6''}), 8.00 (t, 1H, $J = 5.6$ Hz; H⁵), 8.04 (d, 1H, $J = 8.0$ Hz; H^{3''}), 8.09 (d, 1H, $J = 8.0$ Hz; H⁵), 8.38 (t, 1H, $J = 7.8$ Hz; H⁴), 8.49 (m, 2H; H³ + H^{4'}), 8.59 (d, 1H, $J = 8.0$ Hz; H^{3'}) 9.30 (d, 1H, $J = 4.8$ Hz; H^{6'}); minor species δ 1.84 (s, 0.6H, CH₃), 2.37 (dt, 0.4H, $J = 7.6$ Hz; CH₂-3x), 3.07 (dd, A part of an ABX spin system, 0.2H, $J_{AB} = 14.0$ Hz, $J_{AX} = 4.4$ Hz; CH^AH^B-5x), 3.35 (s, 0.2H), 4.20 (pseudo t, broad, $J = 7.6$ Hz; H^{4x}), 7.49 (t, 0.2H, $J = 9.2$ Hz), 7.60 (d, 0.2H, $J = 8.4$ Hz), 7.83 (d, 0.2H, $J = 8.4$ Hz), 8.17 (d, 0.2H, $J = 7.2$ Hz), 8.74 (d, 0.2H, $J = 6.0$ Hz; H⁶). Selected IR bands (ν_{\max} cm⁻¹): 3620 ν (OH), 3403 and 3271 ν (NH), 1726 and 1652 ν (C=O), 1601 ν (C=C) + ν (C=N), 1531 ν (C=O), 1236, 845 ν (PF₆). UV-Vis [CH₃CN, λ_{\max} /nm]: 256sh, 327. Emission spectrum, (λ_{em} nm) = 357.

Synthesis of the gold(I) complex

[Au(C₂ArNHCOQ)(PPh₃)] (10). To a stirred solution of [AuCl(PPh₃)] (0.0495 g, 0.1 mmol) in ethanol (5 mL) were added solid HC₂ArNHCOQ (0.0289 g, 0.1 mmol) and an ethanol solution of tBuOK (0.0224 g, 0.2 mmol). The reaction mixture was stirred at room temperature for 24h. The resulting solution was evaporated to dryness and the yellow solid was recrystallized from dichloromethane/diethyl ether to give the analytical sample Yield 40 %; mp. 200 °C (dec) Anal. Calcd for C₃₆H₂₅AuNO₃P: C, 43.19; H, 3.00; N, 3.47%. Found: C, 43.05; H, 2.97; N, 3.41%. ¹H

NMR (CD₂Cl₂): δ 7.46 (d, 2H, *J* = 8.0 Hz; H^m), 7.50 (d, 1H, *J* = 8.4 Hz; H⁶), 7.52– 7.65 (m, 16H; PPh₃ + H⁸), 7.69 (d, 2H, *J* = 8.0 Hz; H^o), 7.76 (pseudo t, 1H, *J* = 8.4, 7.6 Hz; H⁷), 7.82 (d, 1H, *J* = 7.6 Hz; H⁵), 9.06 (s, 1H; H⁴), 10.86 (s, 1H; NH). Assignments based on Cosy and Noesy experiments. ³¹P{¹H} NMR (CD₂Cl₂): δ 42.2. Selected IR bands (*v*_{max} cm⁻¹): 1713 *v*(C=O), 1100 *v*(PPh₃). UV-Vis [CH₃CN, λ_{max}/nm (ε/M⁻¹cm⁻¹): 238 (sh, 3800), 298 (3980), 302 (4100), 345 (2800). Emission spectrum, (λ_{em} nm) = 434.

X-Ray crystallography

Crystals of **2**-PF₆, **3**-PF₆, and **10** were examined using a Xcalibur Oxford Diffraction diffractometer equipped with CCD area detector and mirror-monochromated Mo Kα radiation (λ = 0.71073 Å). Crystals of **6**-PF₆ were examined using a Bruker Apex II diffractometer, equipped with a CCD area detector and graphite-monochromated Cu Kα radiation (λ = 1.54178 Å). Intensities were integrated from data recorded on 1° (**2**-PF₆, **3**-PF₆ and **10**) or 1.5° (**6**-PF₆) frames by ω or φ rotation. Cell parameters were refined from the observed positions of all strong reflections in each data set. Analytical (**2**-PF₆, **3**-PF₆ and **10**) or multi-scan (**6**-PF₆) absorption correction with a beam profile correction was applied.⁴⁷ The structures were solved by direct methods⁴⁸ (**6**-PF₆ and **10**) or with SHELXT⁴⁹ (**2**-PF₆ and **3**-PF₆) and were refined by full-matrix least-squares on all unique *F*² values,⁴⁸⁻⁵⁰ with anisotropic displacement parameters for all non-hydrogen atoms, and with constrained riding hydrogen geometries; *U*_{iso}(H) was set at 1.2 (1.5 for methyl groups) times *U*_{eq} of the parent atom. The largest features in final difference syntheses were close to heavy atoms and were of no chemical significance. CrysAlis^{Pro} was used for control and integration,⁴⁷ and SHELX⁴⁸ and OLEX2⁵¹ were employed for structure solution and refinement. ORTEP-3⁵² and POV-Ray⁵³ were employed and for molecular graphics. Crystallographic data are reported in Table S2. CCDC 1855896-1855899 contain supplementary crystal data for this article.

Cell viability Assay

The human lung epithelial cancer cells A549, the human ovarian cancer cells SKOV-3, the human breast cancer cells MCF-7 and the human melanoma cells A375 were obtained from ATCC. The human embryonic kidney cells HEK-293 were obtained from Dr. Maria Pia Rigobello (University of Padova). Cells were cultured in DMEM supplemented with 10% FBS and 1% penicillin/streptomycin at 37°C under a humidified atmosphere of 95% air and 5% CO₂. For the evaluation of growth inhibition cells were seeded in 96-well plates at a concentration of 8000 cells per well and grown for 24 h in complete medium. Dilutions of the Au^{III} complexes were freshly prepared from a prepared stock solution (10⁻² M in DMSO) in aqueous media (DMEM). Cisplatin was purchased at Sigma-Aldrich and its stock solutions prepared in aqueous solution (10⁻³ M). After 24 h incubation, 200 μL of the compounds'

dilutions were added to each well to obtain a final concentration ranging from 0 to 50 μM , and the cells were incubated for additional 72 h. Afterwards, medium was removed and 3-(4,5-dimethylthiazol-2-yl)-2,5-diphenyltetrazolium bromide (MTT, Fluorochem) in 10 \times PBS (Phosphate Buffered Saline, Corning) was added to the cells, at a final concentration of 0.3 mg/mL and incubated for 3-4 h. Then, the MTT solution was discarded and replaced with DMSO to allow the formed violet formazan crystals to dissolve. The optical density was quantified in quadruplicates at 550 nm using a multi-well plate reader. The percentage of surviving cells was calculated from the ratio of absorbance of treated to untreated cells. The EC_{50} value was calculated, using GraphPad Prism software, as the concentration causing 50% decrease in cell viability, using a nonlinear fitting of cell viability vs [treatment], and presented as mean \pm SEM of at least three independent experiments.

ESI mass spectrometry

Horse heart cytochrome c (cyt c) was purchased from Sigma (code C7752). Metal complexes / cyt c adducts were prepared in water, with a protein concentration of 50 μM and a gold to protein ratio of 3:1. Metal complexes / amino acids adducts were prepared in water with amino acid (His and Cys) concentration of 150 μM and a gold to amino acid ratio of 1:1 and 1:1:1 for the mix. The reactions were incubated over 24 h and ESI MS spectra recorded at different times (10 min, 3 h, 6 h, 24 h) at room temperature. Samples were analyzed by ESI-QTOF MS on a Water Synapt G2-Si spectrometer by direct infusion at a flow rate of 5 $\mu\text{L min}^{-1}$. The specific conditions used for these experiments were as follows: capillary voltage 2.5 kV, sampling cone voltage 40 V, source offset voltage 80 V, source temperature 120 $^{\circ}\text{C}$, desolvation gas temperature 500 $^{\circ}\text{C}$, cone gas flow 50 L h^{-1} , desolvation gas flow nebulizer flow 6.5 bar.

Capillary Zone Electrophoresis (CZE)–ESI mass spectrometry

Ubiquitin and 3-nitrobenzyl alcohol were purchased from Sigma-Aldrich and the oligonucleotide 5'-dATTGGCAC-3' from Microsynth. Ammonium bicarbonate and formic acid were obtained from Fluka, and methanol and 2-propanol from Fisher. NaOH solution (1 M) was a product of Agilent Technologies. Ultrapure water was received from a Millipore Advantage A10 system (18.2 $\text{M}\Omega$, ≤ 5 ppb TOC, 185 UV). Stock solutions of ubiquitin and the single-stranded DNA-oligomer (200 μM each) were prepared in water. The gold complex **10H**- PF_6 (20 mM) was dissolved in DMSO and diluted with water to a concentration of 1 mM. The stock solutions were mixed to yield final concentrations of 50 μM for each ub/DNA and 200 μM for the gold complex, and the reaction mixture was incubated at 37 $^{\circ}\text{C}$ at constant shaking (400 rpm) in the dark. Aliquots were taken after 10 min, 1 h and 6 h and stored in the freezer at -20 $^{\circ}\text{C}$ until measurement.

Measurements were performed on a G7100 capillary electrophoresis system (Agilent Technologies, Waldbronn, Germany) equipped with a diode-array detector (190-400 nm) and hyphenated with a coaxial sheath-flow CZE–ESI-MS Sprayer Kit (Agilent Technologies) to a high resolution time-of-flight (TOF) mass spectrometer (maXis 4G UHR-TOF, Bruker, Bremen, Germany). The fused silica capillary (undeactivated, 75 μ m, Agilent Technologies, USA) was cut to a total length of 70 cm, a UV/Vis window was prepared at 23 cm and cleaned with isopropanol before installation. The capillary cassette temperature was set to 25 °C. Capillaries were flushed successively with HCl (1 M, 5 min, 950 mbar), water (1 min), NaOH (1 M, 10 min), water (1 min) and background electrolyte (BGE, 25 mM NH_4HCO_3 , pH 7.9, 20 min). A sheath liquid (isopropanol, methanol, water, formic acid and 3-nitrobenzyl alcohol; 25/25/50/0.2/0.5, v/v/v/v/v) was used to close the electric circuit and help the ionization. The sheath flow of 3 μ L/min was provided by a syringe pump (KDS 1000, KD Scientific Inc., Holliston, USA). Before sample injection, the capillary was rinsed with BGE for 1 min. Samples were injected hydrodynamically for 5 s at 50 mbar. Typical instrument parameters can be found in Table 4. ESI-MS data were analyzed and processed using ESI Compass 1.3 DataAnalysis 4.0 (Bruker Daltonics). The extracted ion electropherograms (EIE) in the figures were obtained by selecting the appropriate mass-to-charge ratio including an offset of ± 0.05 m/z .

Table 4. Typical instrument parameters of the CZE–ESI-MS analysis.

CE system	Agilent G7100
Capillary	fused-silica capillary, i.d. 75 μ m, length 70 cm
Background electrolyte	25 mM NH_4HCO_3 , pH 7.9
Separation Voltage	25 kV
Sample Injection	Hydrodynamic 50 mbar, 5s
ESI-MS system	Bruker maXis qTOF
capillary voltage	4.5 kV
gas flow	0.4 bar
dry gas	4 L min^{-1}
dry heater	180 °C
quadrupole energy	4 eV
collision energy	8.0 eV
ion cooler transfer time	70 μ s
Spectra Rate	1 Hz

Supporting Information

The Supporting Information, including compounds' NMR analysis, photophysical studies, antiproliferative activity data, stability studies by UV-visible spectroscopy, as well as

crystallographic data analysis, is available free of charge on the ACS Publications website at DOI: XXXX.

Acknowledgements

AC acknowledges Cardiff University for funding. MA, AC, MAC, LM, and AZ kindly acknowledge Regione Autonoma della Sardegna (RAS) for the financial support coming from L.R. 7, CRP-78365. MAC thanks the MIUR for financial support coming from Legge 11 dicembre 2016 n. 232. MA thanks the Università degli Studi di Cagliari, Fondazione di Sardegna (FdS) and Regione Autonoma della Sardegna (RAS) (“Progetti Biennali di Ateneo FdS/RAS annualità 2016”) for financial support. FO acknowledges Dr Chris Muryn and the X-ray Crystallography Service of the School of Chemistry at The University of Manchester. Authors acknowledge the Erasmus program for a fellowship to SC. Ms. Brech Aikman is kindly acknowledged for helping recording UV-visible spectra of two of the selected compounds.

References

1. Casini, A.; Sun, R. W.; Ott, I., Medicinal Chemistry of Gold Anticancer Metallodrugs. In *Met. Ions Life Sci.*, 2018; Vol. 18.
2. Zou, T. T.; Lum, C. T.; Lok, C. N.; Zhang, J. J.; Che, C. M., Chemical biology of anticancer gold(III) and gold(I) complexes. *Chem. Soc. Rev.* **2015**, *44*, 8786-8801.
3. Kumar, R.; Nevado, C., Cyclometalated Gold(III) Complexes: Synthesis, Reactivity, and Physicochemical Properties. *Angew. Chem. Int. Ed.* **2017**, *56*, 1994-2015.
4. Lee, C. H.; Tang, M. C.; Wong, Y. C.; Chan, M. Y.; Yam, V. W. W., Sky-Blue -Emitting Dendritic Alkynylgold(III) Complexes for Solution-Processable Organic Light -Emitting Devices. *J. Am. Chem. Soc.* **2017**, *139*, 10539-10550.
5. Currie, L.; Fernandez-Cestau, J.; Rocchigiani, L.; Bertrand, B.; Lancaster, S. J.; Hughes, D. L.; Duckworth, H.; Jones, S. T. E.; Credgington, D.; Penfold, T. J.; Bochmann, M., Luminescent Gold(III) Thiolates: Supramolecular Interactions Trigger and Control Switchable Photoemissions from Bimolecular Excited States. *Chem. Eur. J.* **2017**, *23*, 105-113.
6. Bronner, C.; Wenger, O. S., Luminescent cyclometalated gold(III) complexes. *Dalton Trans.* **2011**, *40*, 12409-12420.
7. Bertrand, B.; Williams, M. R. M.; Bochmann, M., Gold(III) Complexes for Antitumor Applications: An Overview. *Chem. Eur. J.* **2018**, *24*, 11840-11851.
8. Jurgens, S.; Kuhn, F. E.; Casini, A., Cyclometalated Complexes of Platinum and Gold with Biological Properties: State-of-the-Art and Future Perspectives. *Curr. Med. Chem.* **2018**, *25*, 437-461.
9. Bertrand, B.; Casini, A., A golden future in medicinal inorganic chemistry: the promise of anticancer gold organometallic compounds. *Dalton Trans.* **2014**, *43*, 4209-4219.
10. Buckley, R. G.; Elsome, A. M.; Fricker, S. P.; Henderson, G. R.; Theobald, B. R. C.; Parish, R. V.; Howe, B. P.; Kelland, L. R., Antitumor properties of some 2-[(dimethylamino)methyl]phenylgold(III) complexes. *J. Med. Chem.* **1996**, *39*, 5208-5214.
11. Parish, R. V.; Howe, B. P.; Wright, J. P.; Mack, J.; Pritchard, R. G.; Buckley, R. G.; Elsome, A. M.; Fricker, S. P., Chemical and biological studies of dichloro(2-((dimethylamino)methyl)phenyl)gold(III). *Inorg. Chem.* **1996**, *35*, 1659-1666.
12. Jurgens, S.; Scalcon, V.; Estrada-Ortiz, N.; Folda, A.; Tonolo, F.; Jandl, C.; Browne, D. L.; Rigobello, M. P.; Kuhn, F. E.; Casini, A., Exploring the C^NA^C theme: Synthesis and biological properties of tridentate cyclometalated gold(III) complexes. *Bioorg. Med. Chem.* **2017**, *25*, 5452-5460.

13. Bertrand, B.; Spreckelmeyer, S.; Bodio, E.; Cocco, F.; Picquet, M.; Richard, P.; Le Gendre, P.; Orvig, C.; Cinellu, M. A.; Casini, A., Exploring the potential of gold(III) cyclometallated compounds as cytotoxic agents: variations on the C^N theme. *Dalton Trans.* **2015**, *44*, 11911-11918.
14. Sun, R. W. Y.; Lok, C. N.; Fong, T. T. H.; Li, C. K. L.; Yang, Z. F.; Zou, T. T.; Siu, A. F. M.; Che, C. M., A dinuclear cyclometalated gold(III)-phosphine complex targeting thioredoxin reductase inhibits hepatocellular carcinoma in vivo. *Chem. Sci.* **2013**, *4*, 1979-1988.
15. Yan, J. J.; Chow, A. L. F.; Leung, C. H.; Sun, R. W. Y.; Ma, D. L.; Che, C. M., Cyclometalated gold(III) complexes with N-heterocyclic carbene ligands as topoisomerase I poisons. *Chem. Commun.* **2010**, *46*, 3893-3895.
16. Zhang, J. J.; Sun, R. W. Y.; Che, C. M., A dual cytotoxic and anti-angiogenic water-soluble gold(III) complex induces endoplasmic reticulum damage in HeLa cells. *Chem. Commun.* **2012**, *48*, 3388-3390.
17. Wenzel, M. N.; Meier-Menches, S. M.; Williams, T. L.; Ramisch, E.; Barone, G.; Casini, A., Selective targeting of PARP-1 zinc finger recognition domains with Au(III) organometallics. *Chem. Commun.* **2018**, *54*, 611-614.
18. Gabbiani, C.; Mastrobuoni, G.; Sorrentino, F.; Dani, B.; Rigobello, M. P.; Bindoli, A.; Cinellu, M. A.; Pieraccini, G.; Messori, L.; Casini, A., Thioredoxin reductase, an emerging target for anticancer metallodrugs. Enzyme inhibition by cytotoxic gold(III) compounds studied with combined mass spectrometry and biochemical assays. *Medchemcomm* **2011**, *2*, 50-54.
19. Li, C. K. L.; Sun, R. W. Y.; Kui, S. C. F.; Zhu, N. Y.; Che, C. M., Anticancer cyclometalated [Au(III)(C^N^C)L](n+) compounds: Synthesis and cytotoxic properties. *Chem. Eur. J.* **2006**, *12*, 5253-5266.
20. Bertrand, B.; Fernandez-Cestau, J.; Angulo, J.; Cominetti, M. M. D.; Waller, Z. A. E.; Searcey, M.; O'Connell, M. A.; Bochmann, M., Cytotoxicity of Pyrazine-Based Cyclometalated (C^N-PZ^C)Au(III) Carbene Complexes: Impact of the Nature of the Ancillary Ligand on the Biological Properties. *Inorg. Chem.* **2017**, *56*, 5728-5740.
21. Marcon, G.; Carotti, S.; Coronello, M.; Messori, L.; Mini, E.; Orioli, P.; Mazzei, T.; Cinellu, M. A.; Minghetti, G., Gold(III) complexes with bipyridyl ligands: Solution chemistry, cytotoxicity, and DNA binding properties. *J. Med. Chem.* **2002**, *45*, 1672-1677.
22. Messori, L.; Marcon, G.; Cinellu, M. A.; Coronello, M.; Mini, E.; Gabbiani, C.; Orioli, P., Solution chemistry and cytotoxic properties of novel organogold(III) compounds. *Bioorg. Med. Chem.* **2004**, *12*, 6039-6043.
23. Massai, L.; Cirri, D.; Michelucci, E.; Bartoli, G.; Guerri, A.; Cinellu, M. A.; Cocco, F.; Gabbiani, C.; Messori, L., Organogold(III) compounds as experimental anticancer agents: chemical and biological profiles. *Biometals* **2016**, *29*, 863-872.
24. Venugopala, K. N.; Rashmi, V.; Odhav, B., Review on Natural Coumarin Lead Compounds for Their Pharmacological Activity. *Biomed Res. Int.* **2013**, Article963248.
25. Yang, J. J.; Yu, Y. W.; Wang, B. X.; Jiang, Y. L., A sensitive fluorescent probe based on coumarin for detection of cysteine in living cells. *J. Photoch. Photobio. A* **2017**, *338*, 178-182.
26. Signore, G.; Nifosi, R.; Albertazzi, L.; Storti, B.; Bizzarri, R., Polarity-Sensitive Coumarins Tailored to Live Cell Imaging. *J. Am. Chem. Soc.* **2010**, *132*, 1276-1288.
27. Maiore, L.; Cinellu, M. A.; Michelucci, E.; Moneti, G.; Nobili, S.; Landini, I.; Mini, E.; Guerri, A.; Gabbiani, C.; Messori, L., Structural and solution chemistry, protein binding and antiproliferative profiles of gold(I)/(III) complexes bearing the saccharinato ligand. *J. Inorg. Biochem.* **2011**, *105*, 348-355.
28. Roder, C.; Thomson, M. J., Auranofin: Repurposing an Old Drug for a Golden New Age. *Drugs R&D* **2015**, *15*, 13-20.
29. Wenzel, M.; de Almeida, A.; Bigaeva, E.; Kavanagh, P.; Picquet, M.; Le Gendre, P.; Bodio, E.; Casini, A., New Luminescent Polynuclear Metal Complexes with Anticancer Properties: Toward Structure-Activity Relationships. *Inorg. Chem.* **2016**, *55*, 2544-2557.
30. Vergara, E.; Cerrada, E.; Clavel, C.; Casini, A.; Laguna, M., Thiolato gold(I) complexes containing water-soluble phosphane ligands: a characterization of their chemical and biological properties. *Dalton Trans.* **2011**, *40*, 10927-10935.
31. Zhang, L.; Hanigan, M. H., Role of cysteine S-conjugate beta-lyase in the metabolism of cisplatin. *J. Pharmacol. Exp. Ther.* **2003**, *306*, 988-994.
32. Garcia, A. E.; Jalilehvand, F., Aerobic reactions of antitumor active dirhodium(II) tetraacetate Rh-2(CH₃COO)(4) with glutathione. *J. Biol. Inorg. Chem.* **2018**, *23*, 231-239.
33. Dimitrova, M.; Turmanova, S.; Vassilev, K., Complexes of glutathione with heavy metals as catalysts for oxidation. *React. Kinet. Mech. Cat.* **2010**, *99*, 69-78.

34. Kumar, D. N.; Singh, B. K.; Garg, B. S.; Singh, P. K., Spectral studies on copper(II) complexes of biologically active glutathione. *Spectrochim. Acta, Part A* **2003**, *59*, 1487-1496.
35. Artner, C.; Holtkamp, H. U.; Kandioller, W.; Hartinger, C. G.; Meier-Menches, S. M.; Keppler, B. K., DNA or protein? Capillary zone electrophoresis-mass spectrometry rapidly elucidates metallo-drug binding selectivity. *Chem. Commun.* **2017**, *53*, 8002-8005.
36. Cinellu, M. A.; Minghetti, G.; Pinna, M. V.; Stoccoro, S.; Zucca, A.; Manassero, M., Synthesis and characterization of mononuclear amidogold(III) complexes - Crystal structure of [Au(N₂C₁₀H₇(CMe₂C₆H₄)-6)(NHC₆H₃Me₂-2,6)]PF₆ - Oxidation of 4-methylaniline to azotoluene. *Eur. J. Inorg. Chem.* **2003**, 2304-2310.
37. Cinellu, M. A.; Minghetti, G.; Pinna, M. V.; Stoccoro, S.; Zucca, A.; Manassero, M., Replacement of the chloride ligand in [Au(C,N,N)Cl]PF₆ cyclometallated complexes by C, N, O and S donor anionic ligands. *J. Chem. Soc., Dalton Trans.* **1999**, 2823-2831.
38. Cinellu, M. A.; Zucca, A.; Stoccoro, S.; Minghetti, G.; Manassero, M.; Sansoni, M., Synthesis and characterization of gold(III) adducts and cyclometallated derivatives with 6-benzyl- and 6-alkyl-2,2'-bipyridines. *J. Chem. Soc., Dalton Trans.* **1996**, 4217-4225.
39. Cinellu, M. A.; Minghetti, G.; Pinna, M. V.; Stoccoro, S.; Zucca, A.; Manassero, M., The first gold(III) dinuclear cyclometallated derivatives with a single oxo bridge. *Chem. Commun.* **1998**, 2397-2398.
40. Maiore, L.; Aragoni, M. C.; Deiana, C.; Cinellu, M. A.; Isaia, F.; Lippolis, V.; Pintus, A.; Serratrice, M.; Arca, M., Structure-Activity Relationships in Cytotoxic Au-I/Au-III Complexes Derived from 2-(2'-Pyridyl)benzimidazole. *Inorg. Chem.* **2014**, *53*, 4068-4080.
41. Cassano, T.; Tommasi, R.; Nitti, L.; Aragoni, M. C.; Arca, M.; Denotti, C.; Devillanova, F. A.; Isaia, F.; Lippolis, V.; Lelj, F.; Romaniello, P., Picosecond absorption saturation dynamics in neutral [M(R,R'-timdt)(2)] metal-dithiolenes. *J. Chem. Phys.* **2003**, *118*, 5995-6002.
42. Wenzel, M.; Casini, A., Mass spectrometry as a powerful tool to study therapeutic metallo-drugs speciation mechanisms: Current frontiers and perspectives. *Coord. Chem. Rev.* **2017**, *352*, 432-460.
43. Hartinger, C. G.; Groessl, M.; Meier, S. M.; Casini, A.; Dyson, P. J., Application of mass spectrometric techniques to delineate the modes-of-action of anticancer metallo-drugs. *Chem. Soc. Rev.* **2013**, *42*, 6186-6199.
44. Gabbiani, C.; Casini, A.; Kelter, G.; Cocco, F.; Cinellu, M. A.; Fiebig, H. H.; Messori, L., Mechanistic studies on two dinuclear organogold(III) compounds showing appreciable antiproliferative properties and a high redox stability. *Metallomics* **2011**, *3*, 1318-1323.
45. Meier, S. M.; Gerner, C.; Keppler, B. K.; Cinellu, M. A.; Casini, A., Mass Spectrometry Uncovers Molecular Reactivities of Coordination and Organometallic Gold(III) Drug Candidates in Competitive Experiments That Correlate with Their Biological Effects. *Inorg. Chem.* **2016**, *55*, 4248-4259.
46. Artner, C.; Holtkamp, H. U.; Hartinger, C. G.; Meier-Menches, S. M., Characterizing activation mechanisms and binding preferences of ruthenium metallo-prodrugs by a competitive binding assay. *J. Inorg. Biochem.* **2017**, *177*, 322-327.
47. *CrysAlis^{Pro}*. Rigaku Oxford Diffraction Technologies: Yarnton, UK, 2015.
48. Sheldrick, G. M., A short history of SHELX. *Acta Crystallogr. Sect. A: Found. Crystallogr.* **2008**, *64*, 112-122.
49. Sheldrick, G. M., SHELXT - Integrated space-group and crystal-structure determination. *Acta Crystallogr. Sect. A: Found. Crystallogr.* **2015**, *71*, 3-8.
50. Sheldrick, G. M., Crystal structure refinement with SHELXL. *Acta Crystallogr. Sect. C: Cryst. Struct. Commun.* **2015**, *71*, 3-8.
51. Dolomanov, O. V.; Bourhis, L. J.; Gildea, R. J.; Howard, J. A. K.; Puschmann, H., OLEX2: a complete structure solution, refinement and analysis program. *J. Appl. Crystallogr.* **2009**, *42*, 339-341.
52. Farrugia, L. J., WinGX and ORTEP for Windows: an update. *J. Appl. Crystallogr.* **2012**, *45*, 849-854.
53. *POV-Ray*. Persistence of Vision Raytracer Pty. Ltd.: Williamstown, Australia, 2004.

TOC Graphic

A new series of novel (C[^]N[^]N) cyclometalated gold(III) complexes have been characterized for their structural and spectroscopic properties. The compounds anticancer activities have been studied *in vitro* and their reactivity with model biomolecules has been elucidated by mass spectrometry techniques, evidencing an unexpected preference for binding to nucleic acids with respect to proteins and amino acids.

